Assessment of Fatigue and Extreme Loading of Wind Turbines

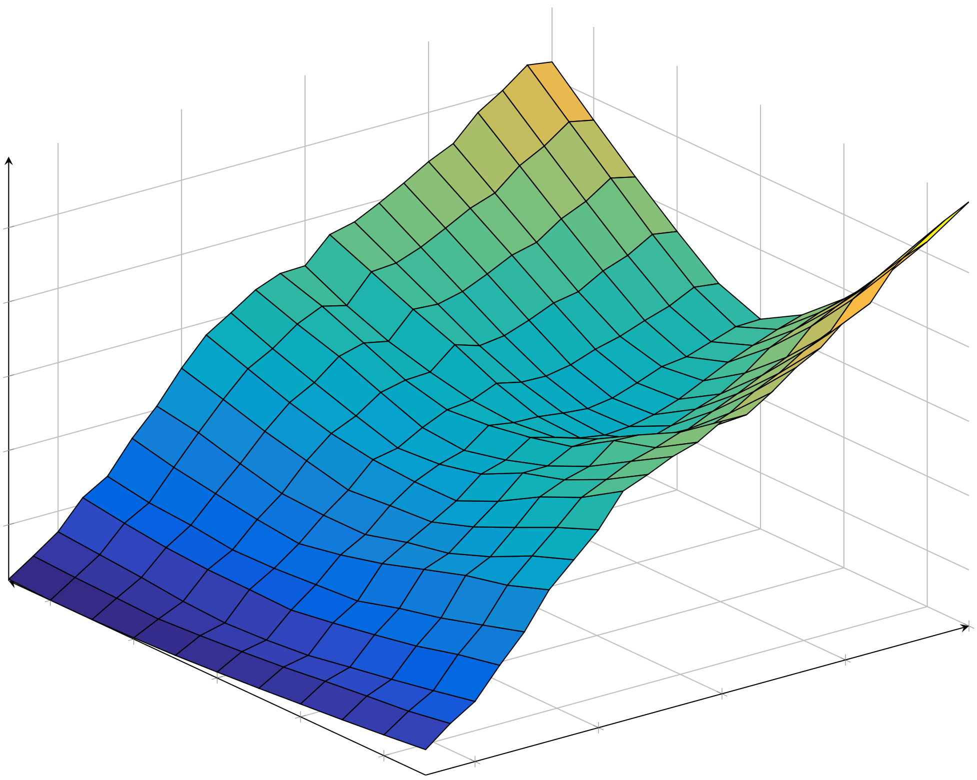

M.Sc. Structural and Civil Engineering
Aalborg Univeristy
4^{th} semester
Group: Fib10-3-15

AALBORG UNIVERSITY
STUDENT REPORT

The faculty of Engineering and Science
Fibigerstræde 10 9000, Aalborg
Telephone: 99 40 84 84
http://www.byggeri.aau.dk

Title: Assesment of Fatigue and Extreme Loading of Wind Turbines
Projectperiod: M.Sc., 4^{nd} semester Spring 2016
Projectgroup: Fib10 3-15
Participants:

Anthon de Luna Søndergaard

Halldór Páll Jóhannsson

Supervisors:
John Dalsgaard Sørensen, Simon Ambühl & Lasse Svenningsen

Circulation: 3
Number of pages: 71
Number of appendixes: 2
Closed the: 09-06-2016

Synopsis:

This protect deals with the assessment of responses of a wind turbine for the IEC-61400 standard D.C.L 1.2 and 1.3. Measured turbulence data at a specific site is distributed with a Lognormal and Weibull distribution to asses which method is more precise. The analysis concluded that the Weibull was a better fit to the turbulence data. Several analysis are done to verify that the output of FAST correspond to the input parameters. In most cases Fast performs as expected.
Load sweeps are done for the NREL 5 MW turbine where different climate parameters variate and assess how the the effect of different climate parameters have on the response. The analysis concluded that the turbulence intensity had the largest effect on the response in comparison with wind shear and the air density.
The NREL 5 MW wind turbine is benchmark against DTU 10 MW wind turbine by comparing the response of both wind turbines. The analysis concluded that the behaviour of the response for the DTU 10 MW wind turbine was similar to the NREL 5 MW turbine, however some inconsistency was between them.
A sensitivity analysis is done to assess the sensitivity of the response models of the different climate parameters. The analysis concluded that the influence of the turbulence intensity had the largest effect on the variance of the response models, compared to the influence of the wind shear and air density.

Preface

This project is written by two students in the 4th semester of the M.Sc. in Structural and Civil Engineering at the Faculty of Engineering and Science at Aalborg University. The theme of the project considers the NREL 5 MW and DTU 10 MW wind turbines and includes developing models dependent on the wind speed. Furthermore this project deals with a detailed load analysis of the DTU 10 MW wind turbine. This report also considers the sensitivity of different climate parameters. The project was conducted in the period from 15-09-2015 to 09-06-2016. The aim of this project is to investigate the different effects from the climate parameters, the behaviour of the turbines and to make load response models for defined load sweeps. For the understanding of this project it is required to have knowledge about the design of wind turbines.

Reading guide

This project contains a main report and two appendices folders, an internal and an external one. The main report focuses on approaches to solve specific problems, assumptions and reflection of the results. The internal appendix folder mainly contains figures and informations while the external appendix folder contains, documents and figures. The Harvard method is used for source references. The book reference is indicated by author, year of publication and publisher. Tables, equations and figures are numbered in accordance with each chapter and sections, if they are without a reference to a source, it has been made by the project group itself. Websites are indicated by title, author, URL and date of download. All the sources have been collected in a bibliography in an alphabetical order.

Contents

Chapter 1

Introduction

Through the last decades there has been an increasing interest of using renewable energy structures due to the global warming and the emission of CO_2. Especially wind as an energy source has been widely accepted and wind turbines today have become larger in size and produce more power. Since 1973 Denmark has rearranged its own energy supply and developed its own production of oil, natural gas and renewable energy source. As a result Denmark has been able to reduce the CO_2 emission with approximately eight percent in the period from 1990-2008. Denmark is a part of the Kyoto protocol and has committed to reduce the emission of the CO_2 even further. Denmark is committed to the EU climate goal which means that at least thirty percent of the total energy consumption should come from renewable energy. [Energi Styrelsen, 2015]

Denmark applies onshore and offshore wind turbines for power production. However the design procedure of a wind turbine onshore is different from an offshore wind turbine since the site conditions are very different. For offshore wind turbines the hydrodynamic loads become important and can in some cases even be the design driver. Wind turbines are designed according to the requirements in standards. However among companies it is still discussed how to access the extreme turbulence loading in extreme wind conditions for the design load case 1.3 in IEC 61400-1 ed. 3 standard during power production.

This project carried out in cooperation with EMD International A/S which is a company developing a software tool, WindPRO, for planning and projecting of wind farms. EMD wishes to further expand the load modelling and are offering students the possibility to cooperate on specific items regarding structural load modelling from aero elastic forces on wind turbines.

The focus of this report is to investigate the structural extreme load response for wind turbines by running several simulations of an aero elastic model in FAST under different extreme conditions. This leads to the following problem statements:

- How is the relation between the structural extreme load response of the wind turbine and the climate parameters under the different extreme wind conditions? Is it possible to establish simple models to determine the structural response without running an aero elastic model.

Besides extreme loading, fatigue load assessment is also a design requirement which also has to be taken into account according to the design load case 1.2 in IEC 61400-1 ed. 3. This report will also investigate the fatigue load responses for the DTU 10 MW turbine. This lead to the following statement:

- What are the differences of the fatigue load response for different components between the DTU 10 MW turbine and the NREL 5 MW turbine?

Chapter 2

Project description

This report contains an analysis of how large a difference there is if a Lognormal or a Weibull distribution is applied for distribute the standard deviation of turbulence measured at a specific site. The data given from EMD A/S gives the basis of the numerical values that should be used for the load sweeps.

The simulations done for this project where made by use of FAST (Fatigue, Aerodynamics, Structures, and Turbulence), which is an open software made by National Renewable Energy Laboratory (NREL). The report contains a section of different analysis based on the simulations. A convergence analysis is performed for different grid points. A verification of the turbulence intensity is done to examine if FAST apply the right turbulence intensity. The components applied are listed in Table 2.4.

Several simulations are done in FAST with different load sweeps and an assessment of which an effect the climate parameters have on the load responses. The considered climate parameters are listed in Table 2.2. The load sweeps are performed for different climate parameter combinations. The individual climate parameter range is divided into specific intervals. These interval are defined by observing measured data from a certain location and calculate the statistical moments of the data. The purpose of performing several load sweeps is to understand how the wind turbine itself reacts when the climate parameters variate under power production.

An analysis of different seeds is performed to investigate the statistical uncertainty in FAST. A seed is defined as a specific number used as an initial condition for generating random wind fields. However some seeds results in unreliable results meaning that the output of FAST is not corresponding to what have been used as an input for FAST.

The NREL 5 MW wind turbine will be benchmarked against the DTU 10 MW wind turbine for design load case (DLC) 1.2 corresponding to a fatigue analysis. The purpose of this analysis is to observe if the two wind turbines react in the similar way or if there is a difference. Load sweeps done for the NREL 5 MW turbine are also performed with the DTU 10 MW turbine and the results from the two turbines are analysed.

Finally a more elaborated sensitivity analysis is performed to study the uncertainty of the response models from the influences of the climate parameters.

A flowchart of the project can be seen in Figure 2.1.

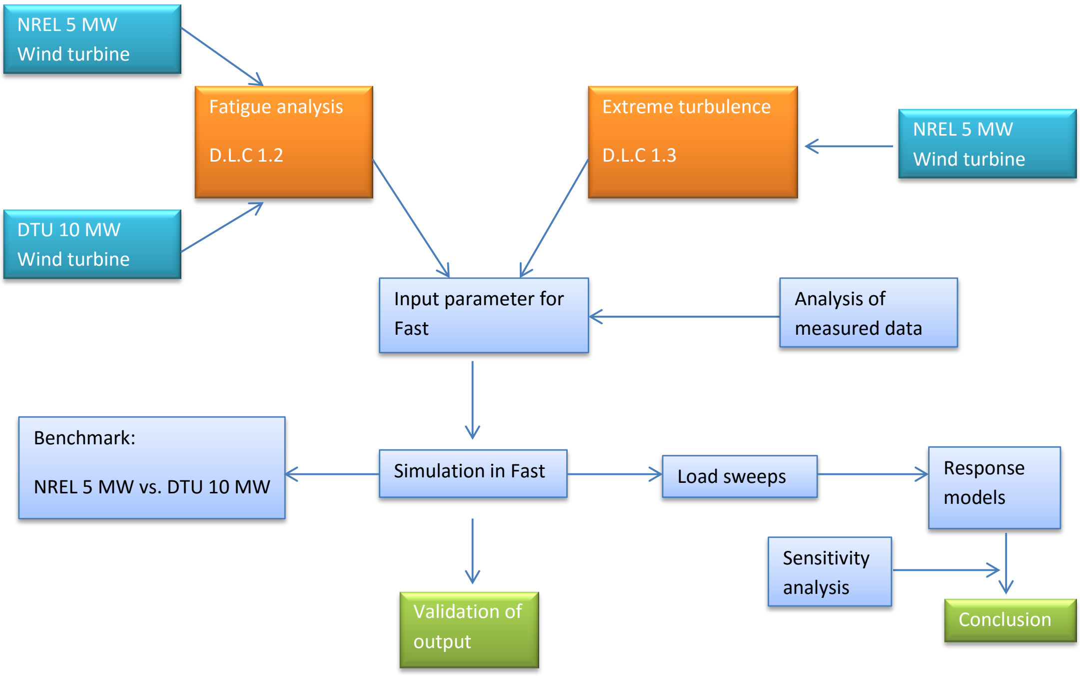

Figure 2.1: Process of the project.

2.1 DCL and input parameters for FAST

For DLC 1.1 and 1.2 a normal turbulence model will be applied due to the different wind conditions and for design load case 1.3 an extreme turbulence model will be applied.

Table 2.1: DLC. [IEC, 2005]

DLC	Wind conditions	Type of analysis
1.1	NTM $V_{in} < V_{hub} < V_{out}$	U
1.2	NTM $V_{in} < V_{hub} < V_{out}$	F
1.3	ETM $V_{in} < V_{hub} < V_{out}$	U

To perform the simulation of the load response of the wind turbine an aero elastic model in the open source code FAST will be applied. The considered code consist of the three programs for an onshore wind turbine:

- TurbSim - Simulation of wind fields.
- AeroDyn - Computation of aerodynamics forces using BEM theory and dynamics stall models.

- FAST - Combined modal and multi-body for estimating the structural response.

Climate parameters

In order to evaluate the extreme and fatigue load of a wind turbine, load sweeps will be analysed by modifying different climate parameters to investigate their effects on the structural response. These parameters are listed in Table 2.2.

Table 2.2: Climate Parameters.

Mean wind speed	V [m/s]
Turbulence intensity	I [%]
Power law exponent	α [−]
Air density	ρ [kg/m^3]

The mean wind speed is defined as the mean wind speed in a certain time interval. For this project the time interval is 10 minutes. The turbulence intensity is defined as the ratio of the standard deviation of the turbulence, σ and the mean wind speed at hub height, V_{hub}, see Equation (2.1).

$$I = \frac{\sigma}{V_{hub}} \tag{2.1}$$

In IEC-61400 ed.3 different wind turbine classes are defined when designing a wind turbine. These classes can be seen in Table 2.3.

Table 2.3: Basic parameters for wind turbine classes. [IEC, 2005]

Wind turbine class	I	II	III	S
V_{ref} [m/s]	50	42.5	37.5	
A I_{ref}[-]	0.16			Values specified by the designer
B I_{ref}[-]	0.14			
C I_{ref}[-]	0.12			

where:

V_{ref}	Reference wind speed average over 10 min [m/s]
A	Designates the category for higher turbulence characteristics [-]
B	Designates the category for medium turbulence characteristics [-]
C	Designates the category for lower turbulence characteristics [-]
I_{ref}	Expected value of the turbulence intensity at 15 m/s

It is seen from Table 2.3 that there are nine combinations in all when designing a wind turbine. However it is required by IEC 61400 that if the turbulence intensity at the specific site exceeds the given values in Table 2.3 to run an aero elastic simulation to obtain the response and an analytical solution is insufficient. The numerical values for the classes can be seen in Figure 2.2

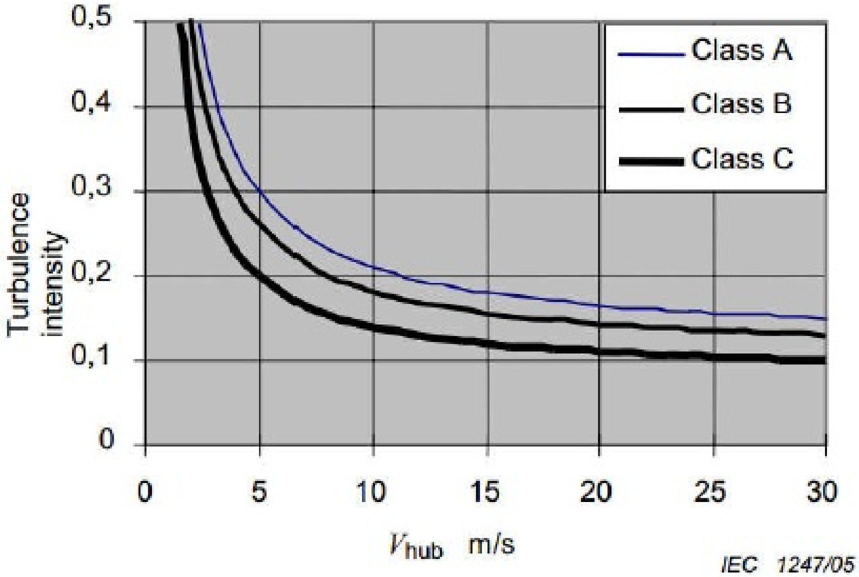

Figure 2.2: Turbulence intensity for the normal turbulence model (NTM). [IEC 61400]

In order to obtain a wind profile which describes the variation of the mean wind speed as a function of the height, the power law wind profile is applied, see Equation (2.2). Since the wind profiles is depended on the atmospheric stability conditions the wind profile will change between day and night. The shape of the wind profile depends on the power law exponent. Failures of blades due to wind shear have occurred, see e.g. Sørensen [2005]. In Figure 2.3 wind profiles with different power law exponents are shown.

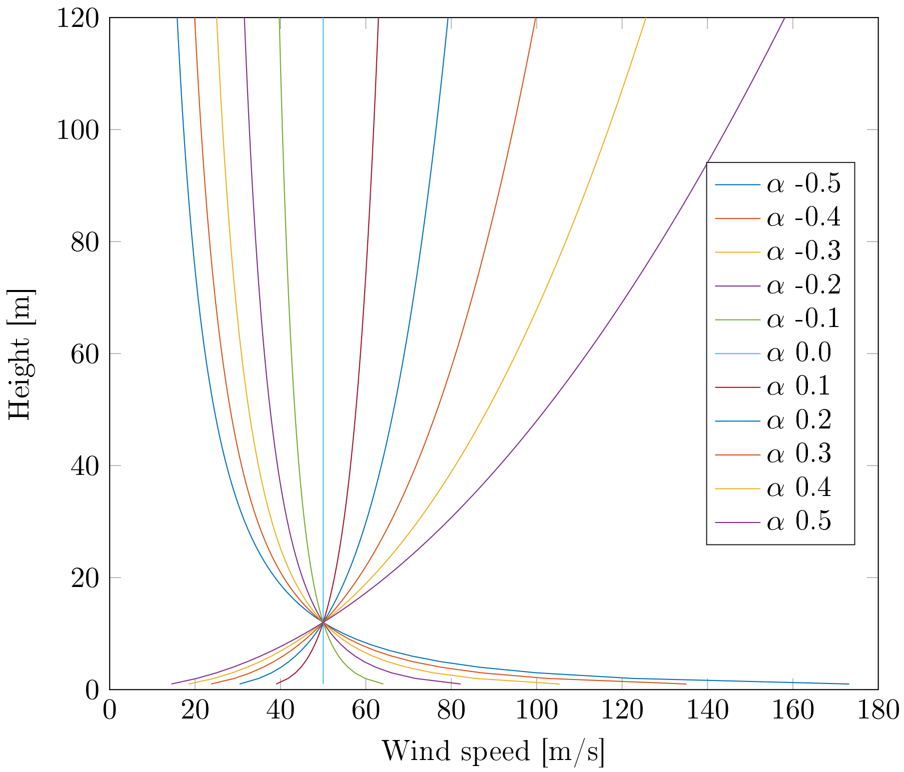

Figure 2.3: Wind profiles with different power law exponents.

$$V(z) = V_{hub} \left(\frac{z}{z_{hub}} \right)^{\alpha} \tag{2.2}$$

Where:

z	Height above the ground [m]
z_{hub}	Hub height of the wind turbine [m]

The air density depends on the temperature and atmospheric pressure. The air density can be determined from the absolute measured temperature (Kelvin) and the measured air pressure. The relation is given in Equation (2.3).

$$\rho_{10,min} = \frac{B}{RT} \tag{2.3}$$

Where:

R	Gas constant [J/kg/°K]
T	Absolute temperature [K]
B	Air pressure [Pa]

In Arctic regions the air density may obtain higher values in contrast to tropic regions. Since the aerodynamic forces are dependent on the air density it is relevant to investigate the effect of various air density when estimating the load response of the wind turbine. [Sørensen, 2005]

In FAST it is possible to get the response from different components of the wind turbine. However since it is not necessary to analyse the response of all components a few are selected. Those are shown in Table 2.4 and are applied throughout the report. Those components are applied because public articles have done similar analysis with these components making it easier to compare the results in this report.

Table 2.4: Considered components in this project.

Load sensor	Description	Unit
RootMyb1	Blade root flapwise bending moment	[kNm]
RootMxb1	Blade root edgewise bending moment	[kNm]
TwrBsMyt	Tower bottom for-aft bending moment	[kNm]
LSSGagMxa	Low speed shaft torque	[kNm]

Chapter 3

Assessment of turbulence data

The newest version of IEC 614000 ed4 recommends that the standard deviation of the turbulence should be Weibull distributed. However the older version recommended to apply the Log-normal distribution. The purpose of this section is to analyse how measured data fits best to one of the distribution function and observe the difference between the two distributions functions applied to the data. The measured data has been given from EMD International and is measured in Denmark. The data consist of measured climate parameters, see Table 3.1, measured every 10 minutes over a six year period.

Table 3.1: Measured data given from EMD.

Wind speed (100 m height)	[m/s]
Wind direction	[°]
Turbulence intensity	[%]
Wind shear	[–]
Air density	[kg/m^3]
Temperature	[°C]

The measured turbulence intensities can be seen in Figure 3.1. The high intensity is caused by a low mean wind speed and a sudden increase in the standard deviation. This is due to that the turbulence intensity is defined as the ratio of the standard deviation of the wind over the mean wind speed. Because of the low mean wind speed it is assumed that these values will not be critical.

Figure 3.1: Scatter diagram of the measured turbulence intensity.

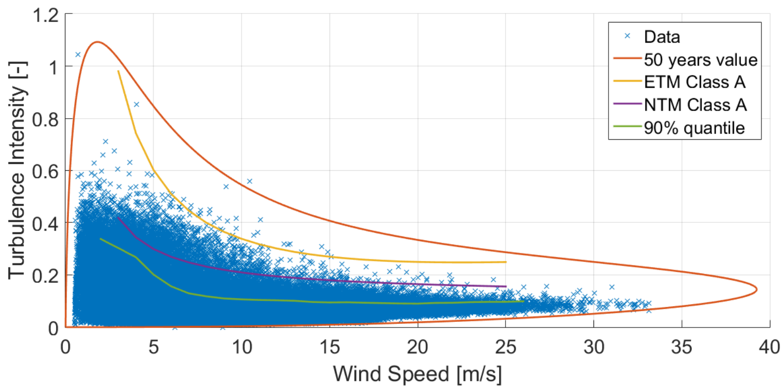

The theory of estimating 50-year values with a return period of 50 years is described in the next section. As the data is from a known location in Denmark there is an option to divide the data dependent on its incoming direction as this location is placed close to the coast line it is possible to investigate the difference in turbulence intensity from wind coming from the sea side and wind coming from the land side of the measured data. According to Figure 3.2, it can be seen that the wind coming from the sea side of the mast is markable higher than from land side. The turbulence intensity seems to follow that conclusion as well.

Figure 3.2: Turbulence data divided by directions.

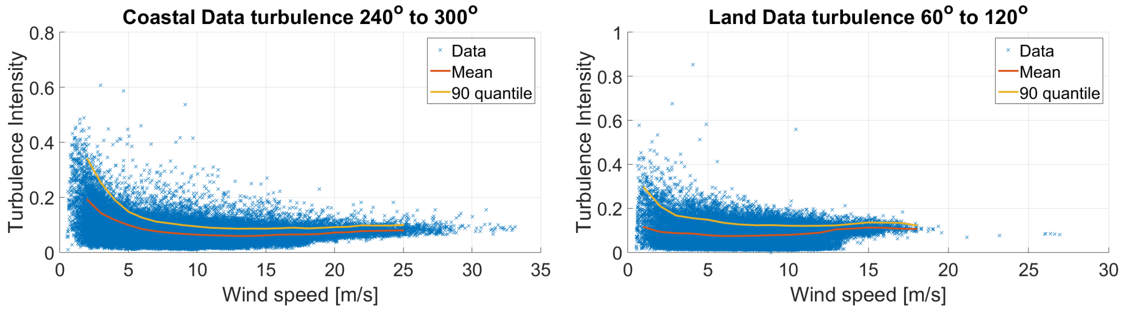

3.1 Enviromental Contour for wind turbines

This section is based on [Fitzwater, 2002]. Before the measured data are distributed an environmental contour line for a 50 year return period has to be determined with a Log-normal distribution for turbulence. The annual distribution of the 10 minute mean wind speed, V, is given by a Rayleigh distribution defined in Equation (3.1):

$$f_v(v) = \frac{2v}{\alpha^2} \exp\left[-\left(\frac{v}{\alpha}\right)^2\right] \tag{3.1}$$

$$\alpha = \frac{2\mu_v}{\sqrt{\pi}} \tag{3.2}$$

Where μ_v is shown in Table 3.2 for wind speed classes I-III.

Table 3.2: Mean value of annual distribution of 10 minute mean wind speed, for wind classes I-III.

Wind Speed Class	V_{ref} [m/s]	μ_V [m/s]
I	50	10
II	42.5	8.5
III	37.5	7.5

3.2 Turbulence Intensity

The standard deviation of the 10 minute wind process is taken as the measure of turbulence, denoted by T. The conditional distribution of turbulence is assumed to follow the Lognormal distribution shown below.

$$f_{T|V}(t|v) = \frac{1}{\sqrt{2\pi}\zeta} \exp\left[-\frac{1}{2}\left(\frac{\ln(t)-\lambda}{\zeta}\right)^2\right] \tag{3.3}$$

The parameters of the lognormal distribution, ζ and λ are defined as:

$$\zeta = \sqrt{\ln(\delta_{T|V}^2 + 1)} \tag{3.4}$$

$$\lambda = \ln(\mu_{T|V}) - \frac{1}{2}\zeta^2 \tag{3.5}$$

with the $\delta_{T|V}$, the conditional coeffecient of variation given as:

$$\delta_{T|V} = \frac{\sigma_{T|V}}{\mu_{T|V}} \tag{3.6}$$

The functions of conditional mean, $\mu_{T|V}$ and standard deviation, $\sigma_{T|V}$ of the turbulence are given by the equations below.

$$\mu_{T|V} = I_{ref}(0.75v + c) \tag{3.7}$$

$$\sigma_{T|V} = 1.44 I_{ref} \tag{3.8}$$

The parameters I_{ref} and c are found in Table 3.3 for turbulence classes A through C.

Table 3.3: Parameters I_{ref} and c for annual conitional distribution of turbulence, for Turbulence classes A-C.

Turbulence Class	I_{ref} [-]	c [m/s]
A	0.16	3.8
B	0.14	3.8
C	0.12	3.8

In order to obtain the contour line for the 50 year return period the windspeed and turbulence have to be transformed from the standard normal space $U_{1,2}$ into the basic space. These equations are given below. The U_1 coordinates of a circle in standard normal space are transformed to the basic space where the wind speed, V, follows a Rayleigh distribution, by first equating the probability values of U_1 and V, in terms of the cumulative distribution functions (CDF) and then solving of v in terms of U_1.

$$\Phi(u_1) = F_v(v) \tag{3.9}$$

$$\Phi(u_1) = 1 - \exp\left[-\left(\frac{v}{\alpha}\right)^2\right] \tag{3.10}$$

$$-\exp\left[-\left(\frac{v}{\alpha}\right)^2\right] = \Phi(u_1) - 1 \tag{3.11}$$

$$\left(\frac{v}{\alpha}\right)^2 = -\ln(1 - \Phi(u_1)) \tag{3.12}$$

$$v = \alpha\sqrt{-\ln(1 - \Phi(u_1)} \tag{3.13}$$

After the first standard normal variable has been transformed to the basic space, the second random variable may be transformed. The derivation of the equation for transforming the second coordinate, U_2, of the circle in standard normal space where the conditional turbulence, T, follows a Lognormal distribution are given below. The CDF are first equated, and then in this case t is found in terms of U_2 and the wind speed dependent on the terms λ and ζ.

$$\Phi(u_2) = F_{T|V}(t,v) \tag{3.14}$$

$$\Phi(u_2) = \Phi\left(\frac{\ln(t) - \lambda}{\zeta}\right) \tag{3.15}$$

$$\ln(t) = u_2\zeta + \lambda \tag{3.16}$$

$$t = \exp\left(u_2\zeta + \lambda\right) \tag{3.17}$$

The contour plot for the standard deviation depending on the wind speed, can be seen in Figure 3.3 for land (direction 60-120°) and for coastal (direction 240-300°).

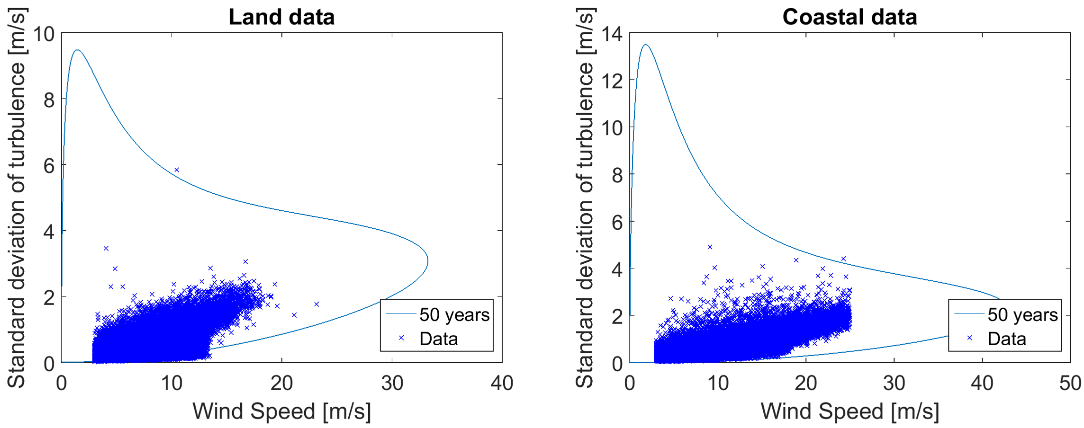

Figure 3.3: Environmental contour for a 50 year return period.

The contour line are used for the data extrapolation. The considered design load cases in this project are D.L.C 1.2 and 1.3. However the results from D.L.C 1.1 are applied for this specific analysis. For D.L.C 1.1 an ultimate analysis is considered meaning that only the extreme values are of relevance. Therefore only the extreme values (approximately 30 values) of the turbulence intensity are extracted and defined by a threshold and fitted to a distribution function. For D.L.C 1.2 an fatigue analysis is considered and all the data will be applied because a large variation of the turbulence intensities may cause to cyclic loading. To insure independence of the extreme values the extreme values are extracted with a minimum interval of 10 steps to insure that the extracted values are the highest in the interval.

The Maximum likelihood method will be applied for both distributions functions. The method is based on the principle of calculating values of parameters that maximize the probability of obtaining the particular sample. The total probability is the product of all individual item probabilities and the product is differentiated with respect to the parameters and the resulting derivatives are set to zero to achieve the maximum. [Ayyub & McCuen, 1997]. The parameters for the distribution functions are then estimated with the Likelihood method. Hereby the estimated values of the turbulence intensity are calculated by using the inverse of the cumulative distributions functions. The non-exceedance probability are calculated with the Weibull plotting positions formula. The 90% confidence interval is applied in both cases. The cumulative distribution function for the Weibull and Lognormal distribution are expressed in Equation (3.18) and Equation (3.19).

$$F = 1 - e^{-\left(\frac{x-B}{A}\right)} \tag{3.18}$$

$$F = \Phi\left(\frac{\ln(x) - B}{A}\right) \tag{3.19}$$

[Liu & Frigaard, 2001] Once the scale and shape parameter for the Weibull distribution,

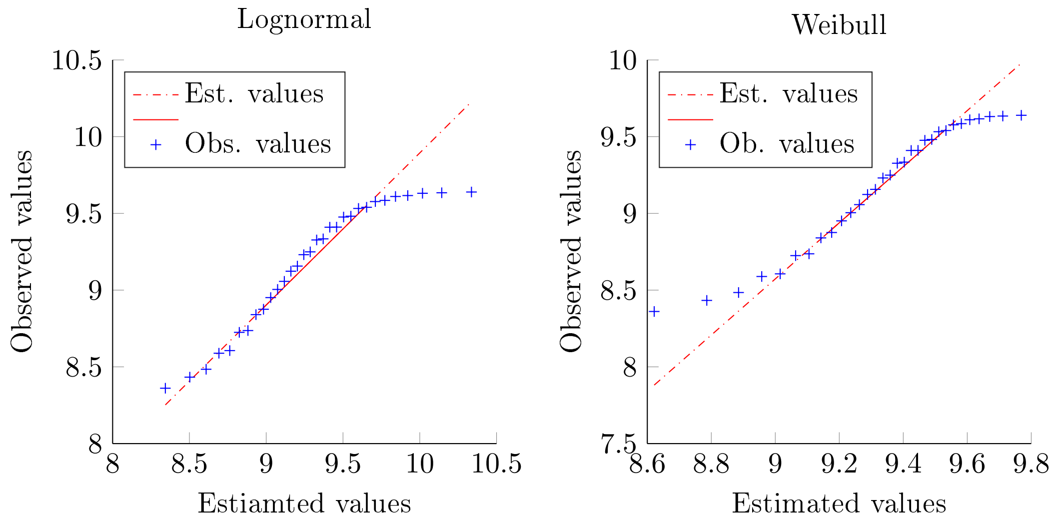

Figure 3.4: QQ-plot for the Log-normal distribution, and Weibull distribution.

the mean and standard deviation values of the Log-normal distribution are determined and the estimated values are plotted against the observed measurements in Figure 3.4.

How well the extreme values are fitted to the distributions function are evaluated with the fitting goodness given in Equation (3.20).

$$E = \frac{1}{n}\sum_{n=1}^{n}\frac{|x_{i,estimated} - x_{i,observed}|}{x_{i,observed}} \tag{3.20}$$

The result can be seen in Table 3.4.

Table 3.4: Measured data.

Distribution function	E [-]
Log-normal	0.026
Weibull	0.020

It is seen in Table 3.4 that the values are very close to each other, however the Weibull distribution fits the data of the turbulence intensities more precisely. As mention before all the data are applied when the D.L.C 1.2 is considered. To make a good visual impression how the data fits a distribution function a CDF is applied, see Figure 3.5.

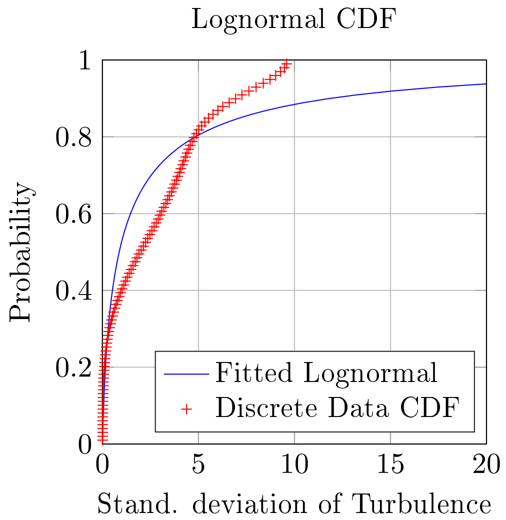

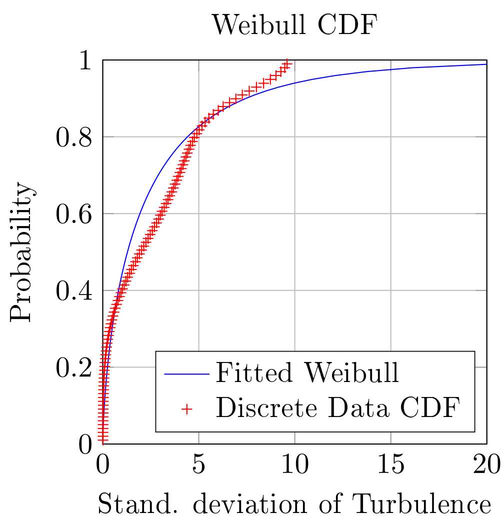

Figure 3.5: CDF of all the data with a Lognormal distribution, Weibull distribution.

It is seen from Figure 3.5 that the Weibull distribution fits the data points better and follow the curve more precisely.

Chapter 4

Analysis of simulations in FAST

FAST generates a simulations that run for 10 minutes and 60 seconds, the first 60 seconds are discarded as they are used to do a stabilization of the model. In FAST there are simulated turbulence fields that are generated by Turbsim input file. The Turbsim input file is where most of the climate parameters for the system can be adjusted i.e turbulence intensity and power law exponent while air density is located in the AeroDyn file, which is part of the FAST tool.

4.1 Description of input parameters to FAST

In the Turbsim input file contains an option, called Meteorological Boundary Conditions, to choose the turbulence intensity by two methods: percentages or by A, B and C where the A, B and C stands for the different turbulence characteristics outlined by the IEC standard.

In the Turbsim input file also the turbulence model type is defined by the IEC standard where e.g NTM stands for Normal Turbulence Model. The wind profile type used is the PL which stands for the Power Law. Time steps and the length of the time series is defined under the Turbine/Model Specifications, see later, along with the grid points in vertical and horizontal dimensions.

4.2 Turbulence intensity, wind shear and air density

In the assessment of the influences from the different factors for the simulation examples are shown to illustrate the changes by altering one parameter at a time. The numerical values are presented in Table 4.1

Table 4.1: Parameters and there numerical values.

Mean wind speed	12	[m/s]
Turbulence Intensity	0.08:0.016:24	[%]
Wind shear	-0.5:0.01:0.5	[–]
Air density	1.25	[kg/m^3]

To see the influences from the different factors, a variation of 15 simulations are done. All simulations run with the same 15 seeds in order to simplify the comparison.

4.3 Convergence analysis for grid points

Simulations with different grid sizes are done to estimate the computational time and differences in resulting maximum load response. The selected components, grid size, the time taken for running 10 simulations and the average of the maximum response for 10 simulations are presented in Table 4.2

Table 4.2: Results for different grid sizes. All responses are in kNm.

Grid size	Time [s]	RootMyb1	RootMxb1	TwrBsMyt	LssGagMxa
6x6	871.7	9949	4664	59491	4233
8x8	906.3	9916	4660	59298	4231
10x10	941.6	9909	4657	59264	4231
12x12	1025.9	9900	4657	59207	4231
14x14	1155.1	9899	4656	59209	4232
16x16	1386.9	9894	4656	59172	4232
18x18	1803.0	9895	4655	59169	4231
19x19	2071.3	9890	4656	59143	4231

The reason that the grid size goes only to 19x19 is because that it is the largest grid size the simulations in TurbSim can generate without changing the Matlab script to account for the allocation of the spectral matrix. It is seen that the time increases with the grid size, while the response does not change significantly. The effect of grid size on the response can be seen in Figure 4.1, the other components are in Appendix A.

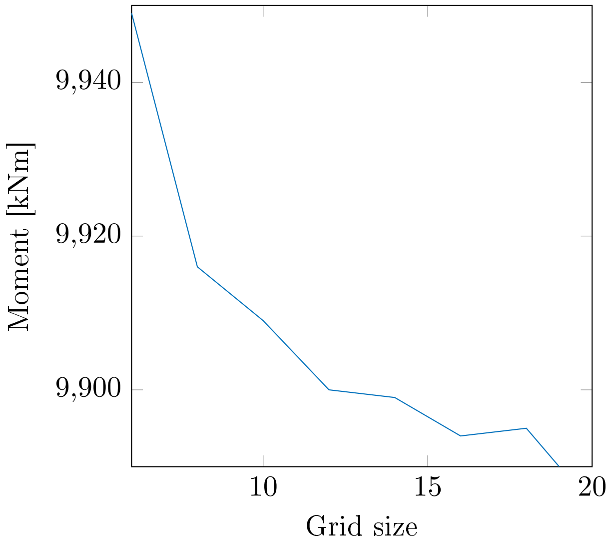

Figure 4.1: RootMyb 1 Response for different grid sizes.

It is seen from Figure 4.1 that the response will decrease while increasing the the grid point. Using grid size of 15x15 was considered to be reasonable as grid above that did not change the responses much, however resulting in more computational time.

4.4 Verifying the Turbulence intensity

The purpose of this section is to verify that FAST generates the correct turbulence intensity. In FAST there is an option to choose the IEC turbulence characteristics in the TurbSim input file under Meteorological Boundary Conditions. In TurbSim there is an option to choose IEC turbulence type and turbulence characteristics.

- IEC turbulence type(NTM=normal, xETM=extreme turbulence, xEWM1=extreme 1-year wind xEWM50=extreme 50-year wind, where x=wind turbine class 1,2 or 3)
- IEC turbulence characteristic (A, B, C or the turbulence intensity in percent) (KHT-EST option with NWTCUP, not used for other models)

One of the complications is that if turbulence models other than NTM is selected, can only be defined by the different turbulence classes A, B, or C.

Running the simulations as NTM models gives the alternative to choose the turbulence intensity as percentiles and FAST generates the time series and attempts to reach the desired turbulence intensity. Occasionally it does not reach the desired turbulence intensity.

As an example for simulated time series for the wind speed 11 m/s can be seen in Figure 4.2.

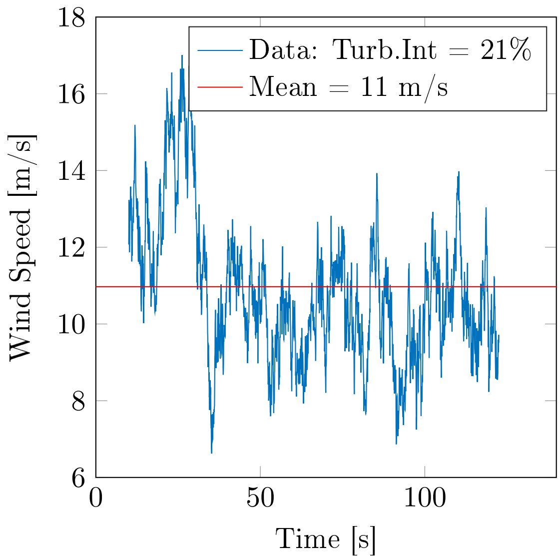

Figure 4.2: Section of simulated time series of wind speed in FAST for mean wind speed 11 m/s.

On Figure 4.2 the applied turbulence intensity is 25 % but the calculated turbulence intensity for Figure 4.2 is 21 % and thereby it can be seen that TurbSim sometimes gives a turbulence intensity which differs from the applied one. A similar figure with mean wind speed 11 m/s can be seen in Appendix A, (see Figure A.5), the applied turbulence intensity is 8 % and computing the actual value gives also 8 %.
As it is difficult to analyse if the desired turbulence intensity was reached by all of the simulations, this is considered to be within, reasonable uncertainty of the software.

4.5 Stabilisation of FAST

In the process of using simulations to calculate the response for wind turbines it is recommended to run the model at least 60 second longer than necessary. This is done to stabilise the model, because as it starts the wind fields uses a stochastic process for the start up phase. Then these 60 seconds are removed from the data. In a small test where the turbulence was set to zero it can be seen how long the model needs to run to stabilise. Figure 4.3 shows the time-dependent RootMyb1 (Blade flapwise moment) for the first 80 seconds. from this figure it can be seen that the extreme response would be higher than after the 60 second which is noted with a red line. A similar figure with wind shear of -0.5 can be seen in Figure A.6.

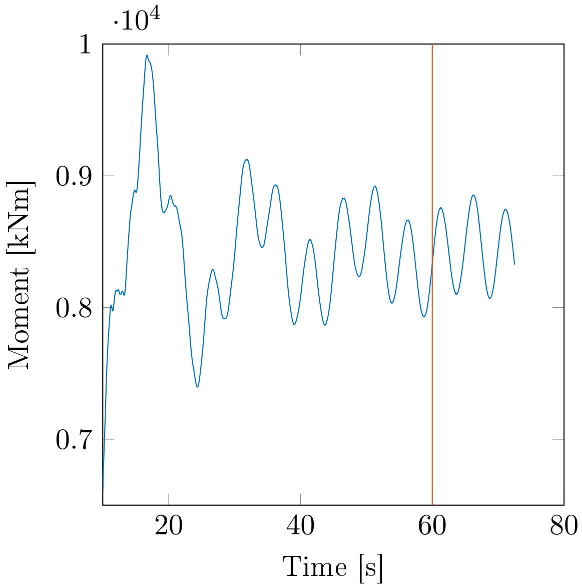

Figure 4.3: Time series for mean wind speed 12 m/s and turbulence intensity of 0, with wind shear of 0.

4.6 Number of simulations

It has been known by user of FAST that some seeds result in unreliable responses it was therefore decided to use 15 seeds for all the simulations.In the simulations made by FAST there is some statistical uncertainty, these can be minimized by increasing the number of simulations and using another random seed. To simplify the analysis, the same random seed is used for each simulation. These seeds are presented in Table 4.3. There are some seeds that have been known to cause issues with FAST i.e the resulting output file generated by FAST is not reliable.

Table 4.3: Seeds used for simulations.

Sim. 1	1280731454
Sim. 2	1362806954
Sim. 3	1583531700
Sim. 4	-1784834451
Sim. 5	-430430244
Sim. 6	-1031348766
Sim. 7	1288784308
Sim. 8	-294575368
Sim. 9	1763717987
Sim. 10	-1366456607
Sim. 11	-1014458748
Sim. 12	-1522398486
Sim. 13	1351727939
Sim. 14	1742863079
Sim. 15	-1602079424

These seeds are tested and a plot was made which shows the mean wind speed together with the maximum and minimum values, (see Figure 4.4). As the number of simulations increases the statistical uncertainty decreases. As IEC 64100 recommends that at least six 10-minute simulations or a continuous 60 minute period should be performed for obtaining reliable data for design load case 1.1. In this report there where 15 simulations performed for each mean wind speed. [IEC, 2005]

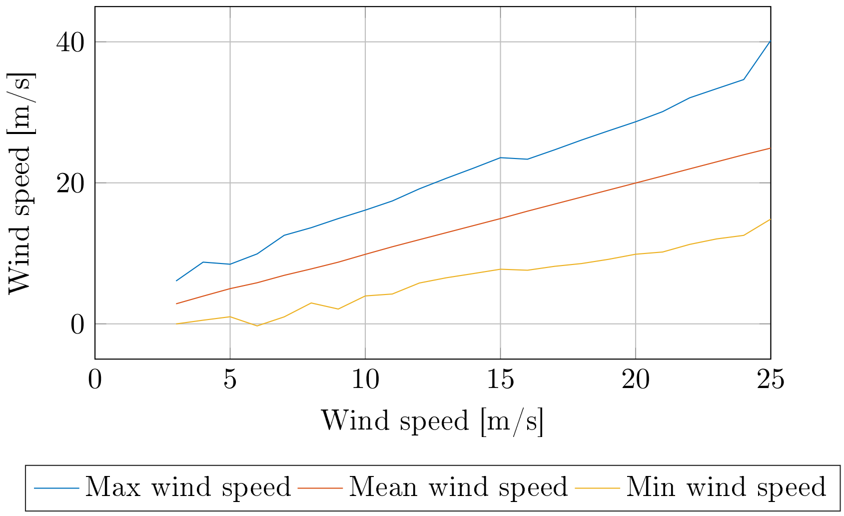

Figure 4.4: Analysis on seed 1.

4.7 Difference of the response between FAST V6 and FAST V8

During this project, a new FAST version (V8) was released. In order to minimize the effort for redoing all simulations, a comparison between the new version V8 and the old FAST version (V6) which is considered in this report, is done. The considered component is the RootMyb1, Flapwise bending moment. The input parameters for Turbsim are shown below. The turbulence intensity has been set to 16 %. A 19 x 19 vertical and horizontal grid-points has been applied for the simulation. The applied wind profile type is the Power Law profile where the wind shear has a variation from –0.5 to 0.5 in order to assess how great an effect the wind shear has on the response.

The response is plotted for a certain value of wind shear as a function of the mean wind speed. It should be mentioned that it is the loads from a 10 min time series that has been used to calculate the response and not the characteristic load for a return period of 50 year which is required for DLC 1.1. The maximum, mean and minimum value of 15 simulations have been computed and are plotted in Figure 4.5.

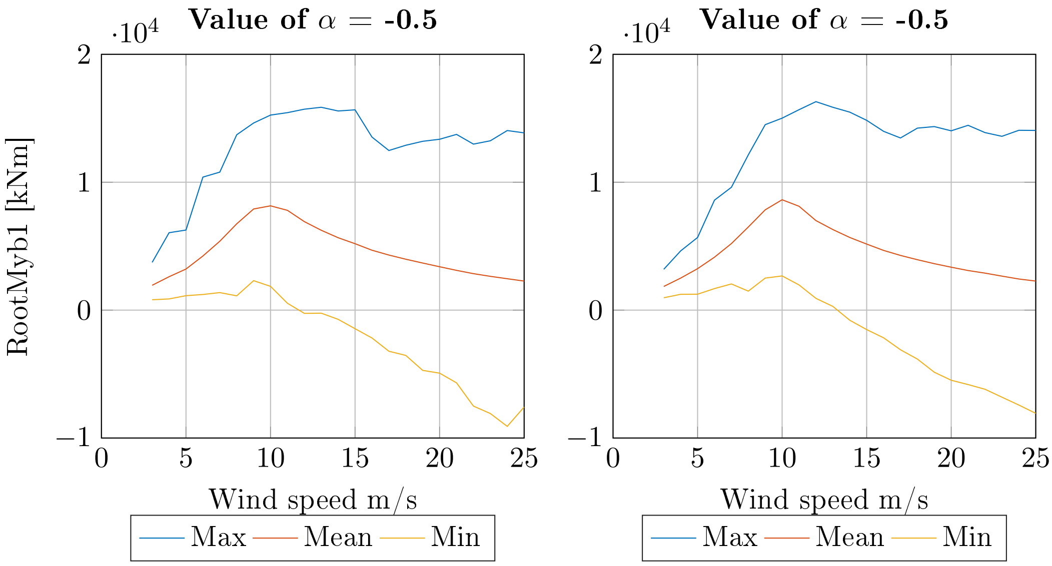

Figure 4.5: RootMyb1, V6 on the left and V8 on the right.

It is seen from Figure 4.5 that the response of the component is not very much different from the two versions. However, it is seen that the trend of the maximum and minimum values is quite different between the two versions, but the mean value seems to be quite similar.

The influence of the turbulence intensity

Another important climate parameter which has an influence on the load response is the turbulence intensity. In this section it is investigated how large effect the turbulence intensity has on the response. In this case the wind shear is equal to 0.2, as recommend in the IEC-61400. 15 simulation has been run for each mean wind speed. The seeds applied are different from each simulation, but the same are applied for each mean wind speed. The response for the component flapwise beding moment is considered and can be observed in the Figure 4.6.

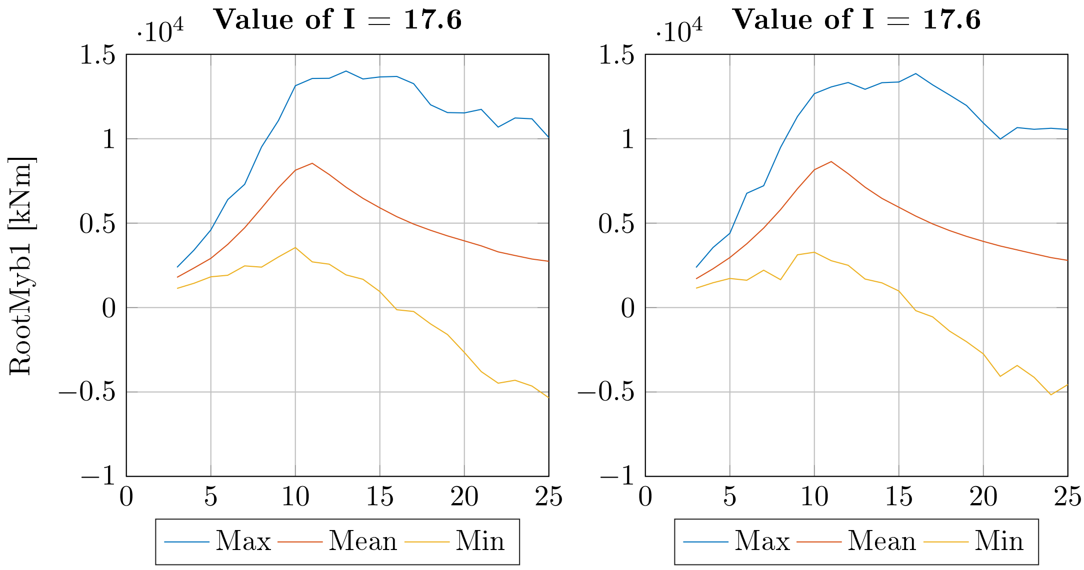

Figure 4.6: RootMyb1, V6 on the left and V8 on the right.

Comparing the plots in Figure 4.5 and 4.6 show that the response values in FAST version 6 versus the FAST version 8 differ. The response from V8 tends to show more extreme values for the maximum and the minimum response and the mean values tends to be quite higher. While both versions show the same tendency to decrease the mean response value after V_{rated}. This effect is expected because pitching the blades reduces the response.

Chapter 5

Response analysis

The purpose of this chapter is to create response surfaces with different load sweeps with focus on a specific climate parameter. The studied climate parameters are mentioned in Chapter 2.1. It is expected that an increase in the turbulence will increase the response linearly and a higher wind speed will have the same effect. Regarding the wind shear it is expected that the response will behave as a second order polynomial, the influence from air density is expected to have a minor effect on the response, see Toft et al. [2000].

5.1 Load sweeps

For the response analysis, certain wind speed where considered, below, around and above rated wind speed these were chosen, as this is were most of the changes in the control take place and where the turbine starts and stops producing power. Load sweeps are performed by changing one climate parameters in a certain interval, for example the turbulence intensity in a interval of 11-91% and keeping the other parameters constant. This interval has been chosen because the turbulence models in IEC recommends it. The turbulence intensity is determined according to the IEC-61400 ed.3. Next the variation of the climate parameters are combined to study how the response behaves. However, there is an uncertainty of the wind shear, but it is assumed that the interval for wind shear is reasonable since the frequency of the wind shear below and above -0.2 and 0.5 respectively is very low. In order to save computational time certain values of the turbulence intensity and wind shear are chosen and it is estimated that these values are sufficient for the response analysis. Another load sweep is performed where the turbulence intensity and air density are combined. The interval for the air density is chosen to 1.1-1.3 which seems reasonable according to previous studies, [Toft et al., 2000]. When the response analysis is done a response model will be done in order to describe the behaviour of the response with a regression model.

The load sweeps that will be simulated can be seen in Table 5.1 and 5.2.

Table 5.1: Load sweeps 1.

Climate parameters					
Wind speed [m/s]	5	11	12	13	24
Turbulence intensity [%]	11	37	64	75	91
Wind shear [-]	-0.2	0.1	0.2	0.3	0.5

Table 5.2: Load sweeps 2.

Climate parameters					
Wind speed [m/s]	5	11	12	13	24
Turbulence intensity [%]	11	37	64	75	91
Air density [kg/m^3]	1.1	1.15	1.2	1.225	1.3

Simulations with three climate parameters are also performed. This is done to analyse how the response is effected of three different climate parameters. The load sweep can be seen in Table 5.1.

Table 5.3: Load sweeps 3.

Climate parameters			
Wind speed [m/s]	5	12	24
Turbulence intensity [%]	11	64	91
Wind shear [-]	-0.2	0.2	0.5
Air density [kg/m^3]	1.1	1.2	1.3

Wind turbine class AI with reference turbulence intensity of 0.16 has been applied for the calculations of the turbulence intensity for the simulation. It should be noticed that high turbulence intensity between 35-91 % will almost never occur for high wind speeds according to the IEC standards and the response at those turbulence intensities can be ignored.

5.2 Design load case 1.1

The response of different components are determined of the wind turbine during power production. DLC 1.1 requires a normal turbulence model defined in the IEC-61400 ed.3 where $V_{in} < V_{hub} < V_{out}$. In order to asses the 50 year characteristic load. A load extrapolation has to be performed, since FAST simulates 10 minutes of response.

5.2.1 Load extrapolation of data

For DLC 1.1 in IEC 61400 ed.3 the response from the 10 minute simulation has to be load extrapolated corresponding to a 50 year characteristic load. The extreme value of the response is extrapolated by the peak over threshold method. The threshold value is according to IEC 61400-1 given by Mean + 1.4 multiplied with the standard deviation. The individual extremes are assumed to be independent with a minimal separation of 10 seconds.

For each mean wind speed a local distribution function for the extremes is determined. The local extremes are usually assumed Weibull distributed, Equation (5.1).

$$F_{local}(l|T,V) = 1 - \exp\left(-\left(\frac{l-\gamma}{\beta}\right)^{\alpha}\right) \tag{5.1}$$

The distribution parameters α, β and γ can be obtain either by the Method of Moments, Least Square and Maximum Likelihood. In this project a 2-parameter Weibull has been applied where the parameters have been determined with the Maximum Likelihood Method.

Then a long-term distribution is performed by integrating over the mean wind speeds during operation, see Equation (5.2).

$$F_{long-term}(l|T) = \int_{V_{in}}^{V_{out}} F_{local}(l|T,V)^{n(v)} f_v(V)dv \tag{5.2}$$

The parameter n(v) is equal to the number of extremes within the time series T at each mean wind speed V.

A draft version of IEC-61400-1, ed.4, suggests two alternative and more robust simpler methods to determine the characteristic value. These two additional alternative are:

a) *The characteristic value is obtained as the largest (or smallest) among the average values of the 10-min extremes determined for each wind speed in the given range, multiplied by 1.35. This method can only be applied for the calculation of the blade root in-plane moment and out-of-plane moment and tip deflection.*

b) *The characteristic value is obtained as the largest (or smallest) among the 99th percentile (or 1st percentile in the case of minima) values of the 10-min extremes determined for each wind speed in the given range, multiplied by 1.2*

In Section 5.1 the response for different components are simulated and illustrated as a function of wind shear and turbulence intensity. The characteristic load will be shown in this section for both the IEC-61400 ed.3 and ed.4 considering flapwise bending moment and edgewise bending moment. Case a.) from ed.4 is considered since this simple extrapolation method can be used for the flapwise and edgewise bending moment. The results are compared against each other.

In Figure 5.1, it is seen that the characteristic load calculated by the method in ed.4 in the considered example predicts higher loads compared to the method in ed.3 with extrapolation.

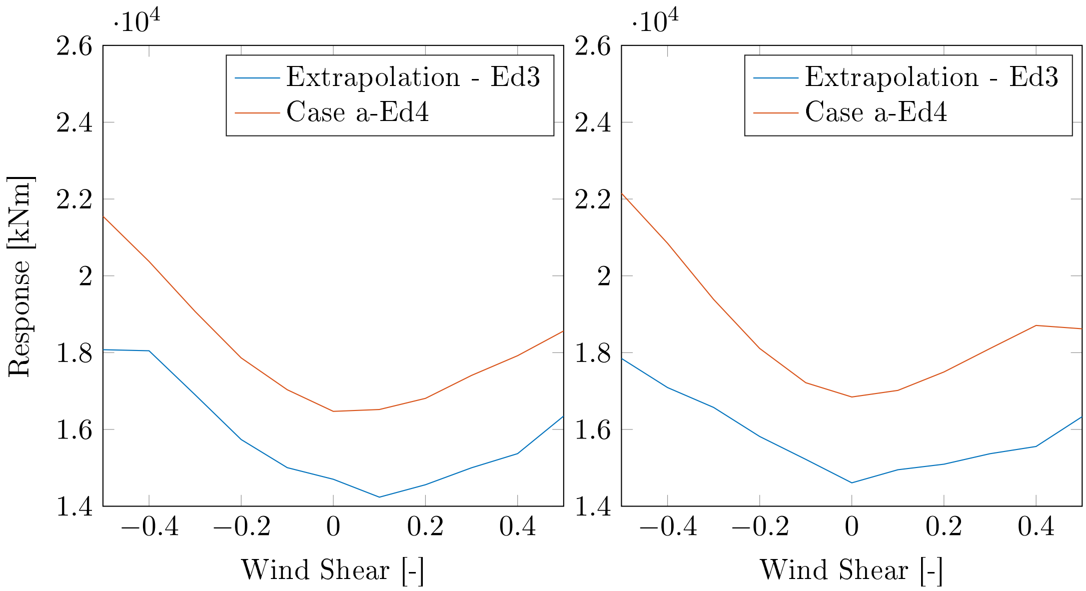

Figure 5.1: Flapwise bending moment on the left and edgevise bending moment on the right.

The new suggested method in IEC-61400 ed.4 predicts higher values of the response compared to ed.3 and seems to be a more conservative method. The ratio between the method in ed.3 and ed.4 are calculated in order to see how much the method in ed.4 overestimates the response. The results can be seen in Table 5.4 and 5.5 for the mean wind speed 25 m/s.

Table 5.4: Response from Ed.3 and Ed.4 and the ratio of the two methods. Component: Flapwise bending moment.

α [-]	-0.5	-0.4	-0.3	-0.2	-0.1	0	0.1	0.2	0.3	0.4	0.5
Ed.3 [kNm]	15.2	14.1	12.9	12.2	11.4	10.9	11.0	11.4	11.9	12.2	13.3
Ed.4 [kNm]	16.9	15.5	13.8	12.6	12.0	11.5	11.3	12.0	12.8	13.6	14.3
$\frac{Ed.4}{Ed.3}$ [-]	1.11	1.10	1.06	1.03	1.05	1.05	1.03	1.06	1.08	1.12	1.08

Table 5.5: Response from Ed.3 and Ed.4 and the ratio of the two methods. Component: Edgewise bending moment.

α [-]	-0.5	-0.4	-0.3	-0.2	-0.1	0	0.1	0.2	0.3	0.4	0.5
Ed.3 [kNm]	17.3	14.6	14.2	12.6	11.0	11.1	11.9	12.5	13.1	13.9	15.7
Ed.4 [kNm]	18.6	15.7	14.9	13.4	11.7	11.52	11.9	12.8	13.7	14.6	17.0
$\frac{Ed.4}{Ed.3}$ [-]	1.07	1.07	1.05	1.06	1.06	1.03	1.00	1.02	1.04	1.05	1.09

A similar assessment has been performed where the response is a function of the turbulence intensity. The interval of the turbulence intensity was in section 5.1 defined between 11 and 91 %. However for this analysis the turbulence intensity is limited to 24 % since the only purpose of this analysis is to assess the difference between the two methods. Flapwise bending moment and edgewise bending moment are again the considered components and are shown in Figure 5.2 dependent on different turbulence intensity values.

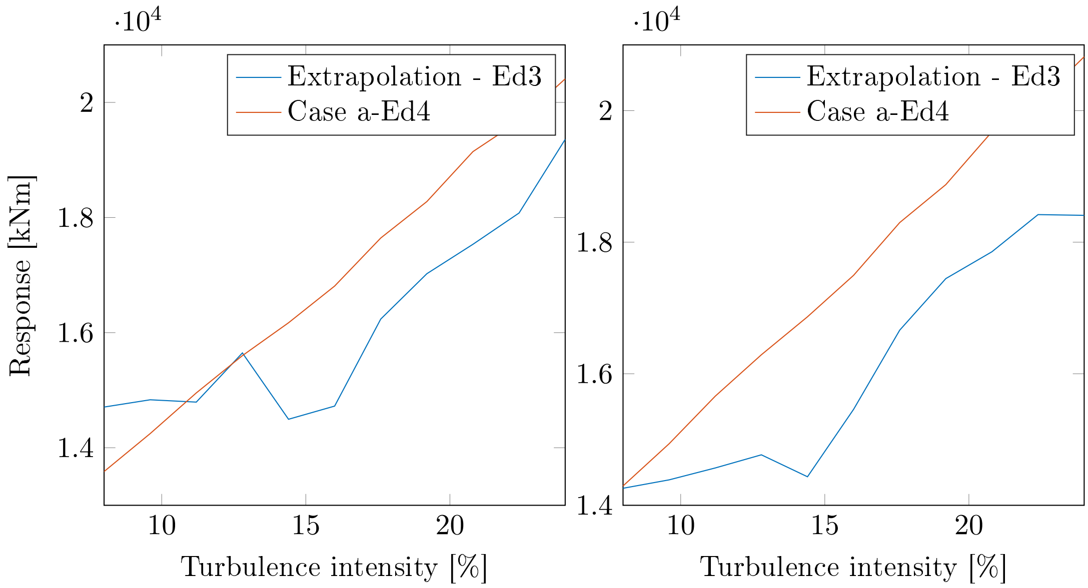

Figure 5.2: Flapwise bending moment on the left and Edgevise bending moment on the right.

The response determined from the two methods are again normalized with respect to each other and can be seen in Table 5.6 and 5.7.

Table 5.6: Response from Ed.3 and Ed.4 and the ratio of the two methods. Component: Flapwise bending moment.

I_{ref}[%]	8	9.6	11.2	12.8	14.4	16	17.6	19.2	20.8	22.4	24
Ed.3 [kNm]	14.7	14.8	14.8	15.6	14.5	14.7	16.2	17.0	17.5	18.1	19.4
Ed.4 [kNm]	13.6	14.2	15.0	15.6	16.2	16.8	17.6	18.3	19.1	19.7	20.4
$\frac{Ed.4}{Ed.3}$ [-]	0.92	0.96	1.01	1.00	1.12	1.14	1.09	1.07	1.09	1.09	1.05

Table 5.7: Response from Ed.3 and Ed.4 and the ratio of the two methods. Component: Flapwise bending moment.

I_{ref}[%]	8	9.6	11.2	12.8	14.4	16	17.6	19.2	20.8	22.4	24
Ed.3 [kNm]	14.2	14.4	14.6	14.8	14.4	15.5	16.7	17.4	17.9	18.4	18.4
Ed.4 [kNm]	14.3	14.9	15.7	16.3	16.9	17.5	18.3	18.9	19.7	20.1	20.8
$\frac{Ed.4}{Ed.3}$ [-]	1.00	1.03	1.07	1.10	1.17	1.13	1.09	1.08	1.10	1.09	1.13

From this section it is concluded that the new method proposed in IEC-61400 ed.4 estimates a larger response compared to method for load extrapolation in IEC-61400 ed.3 for both cases of variation of wind shear and turbulence intensity when considering DLC 1.1. The response behaves different when wind shear is divided into an interval and shows an parabolic shape while it is seen that increasing the turbulence intensity the response increases almost linearly. This conclusion corresponds well from previous results from [Toft et al., 2000].

5.3 Design load case 1.2

For D.L.C 1.2, a fatigue assessment is considered. The response is determined during power production. Similar to D.l.C 1.2 a normal turbulence model defined in IEC-61400 ed.3 is applied where $V_{in} < V_{hub} < V_{out}$. The limit state is reached when the accumulated damage exceeds one when Miner's rule is applied.

5.3.1 Fatigue Assessment

The fatigue damage of wind turbine is asses by counting the cyclic loading of a wind turbine when it is exposed to a daily variation of the wind during its life time. One of the most common and used counting method is the rainflow counting. The reason why the rainflow counting is mostly preferred to apply is due to fact that it takes the large stress range into account which will results in larger fatigue damage. The main idea behind the rainflow counting is to apply the stress-time or strain history history such that the time axis is plotted vertically downwards and represents a raindrop falling down the roof. The rules of the rainflow counting are listed below:

1. Based on the real spectrum, draw a stylistic spectrum which only takes the sequence of the loads and their magnitudes into account.
2. The stylistic spectrum is imagined to be a "roof" and it starts raining on both the inside and the outside of the roof.
3. The stylistic spectrum is drawn with the time axis rotated to a vertical direction and positive downwards

4. The flow of the rain drops are controlled by the following rules:
   (a) The drops start running from the top of the roof and each drop must finish before the next starts.
   (b) If a drop "meets" another drop coming from a higher point on the roof, the "lower" drop stops.
   (c) The drops continue to run down the roof unless: Either the following peak (or valley if the drop started at a valley) is equal to or larger than the peak (or valley) it is initiated from.
5. Repeat these steps for all peaks/valleys

Each drops path from initiation until stop corresponds to the stress (or strain) range corresponding to one reversal. The stress (or strain) ranges are grouped in suitable intervals and the total number of cycles in each interval corresponds to half the number of reversal in each interval. [Schjødt-Thomsen, 2015]

Once the stress ranges are counted and rearranged into intervals the number of cycles to failure for a given stress level can be estimated from the SN-curve, see Equation (5.3).

$$log(N_i) = log(K) - m \cdot log(\Delta\sigma_i) \tag{5.3}$$

where:

N_i	Number of cycles to failure [Cycles]
$\Delta\sigma_i$	Stress range [MPa]
m	Wöhler exponent [-]
K	Material constant [-]

The Wöhler exponent for the considered components in this report are given in Table 5.8.

Table 5.8: Wöhler exponent for components.

Component	Wöhler exponent
RootMyb1	10 [-]
RootMxb1	10 [-]
TwrBsMyt	4 [-]
LSSGagMxa	6 [-]

The fatigue load is then estimated based on Miner's rule for linear damage accumulation. The fatigue loading can therefore be expressed by the Damage Equivalent load (DEL) which for a specific mean wind speed V_j, turbulence $\sigma_{1,j}$, wind shear α_j and air density ρ_j is determined by Equation (5.4).

$$DEL(V_j,\sigma_{1,j},\alpha_j,\rho_j) = \sqrt[m]{\frac{1}{N_{eq}}\sum_i n_i(\Delta F_i)^m} \tag{5.4}$$

where:

n_i	Number of load cycles within stress range ΔF_i [-]
N_{eq}	Equivalent number of load cycles equal to 10^{10} [MPa]

The damage equivalent load from different time periods and wind climate parameters can be combined in Equation (5.5)

$$F_{DEL} = \sqrt[m]{\sum_j w(V_j,\sigma_{1,j},\alpha_j,\rho_j)\cdot DEL(V_j,\sigma_{1,j},\alpha_j,\rho_j)^m} \tag{5.5}$$

where w is a weight factor specifying the probability of occurrence for the wind climate parameters.

5.4 Design load case 1.3

For D.L.C 1.3 a 50 year extreme turbulence from the time series are applied in order to obtain the 50 year characteristic load of the response (ultimate analysis) during power production. For this D.L.C there is no need for a load extrapolation. However this design load case requires the extreme turbulence model as input for turbulence generator where $V_{hub} < V_{out}$ and since extreme turbulence is applied there is no need for a load extrapolation of the extreme events. The results from the DLC 1.3 is expected to be the same as the results from DLC 1.1 and in common practice the results from DLC 1.3 are calibrated from the results from DLC 1.1.

5.5 Response surfaces & Response models

In this section the simulated response surfaces and response models are presented. The load sweeps applied are given in Table 5.1. The considered components are given in Table 2.4 (p. 10).

The central composite design has been applied to create the response models. The regression parameters are in Appendix B.

The regression model which accounts for the second order terms and interaction is given by Equation (5.6).

$$f(x) = \beta_0 + \sum_{i=1}^{k} \beta_i X_i + \sum_{i=1}^{k} \sum_{j \geq i}^{k} \beta_{ij} X_i X_j \tag{5.6}$$

where β_i and β_j are regression parameters. Equation Equation (5.6) can be written in matrix form Equation (5.7).

$$f = X\beta \tag{5.7}$$

$$f = \begin{bmatrix} f_1 \\ f_2 \\ \vdots \\ f_n \end{bmatrix} \tag{5.8}$$

$$X = \begin{bmatrix} 1 & x_{1,1} & x_{1,2} & \dots & x_{1,k} & X_{1,1}X_{1,1} & X_{1,1}X_{1,2} & \dots & X_{1,k}X_{1,k} \\ 1 & x_{2,1} & x_{2,2} & \dots & x_{2,k} & X_{2,1}X_{2,1} & X_{2,1}X_{2,2} & \dots & X_{2,k}X_{2,k} \\ \vdots & \vdots & \vdots & \ddots & \vdots & \vdots & \vdots & \ddots & \vdots \\ 1 & x_{n,1} & x_{n,2} & \dots & x_{n,k} & X_{n,1}X_{n,1} & X_{n,1}X_{n,2} & \dots & X_{x,k}X_{n,k} \end{bmatrix} \tag{5.9}$$

$$\beta = \begin{bmatrix} \beta_0 \\ \beta_1 \\ \beta_2 \\ \vdots \\ \beta_k \\ \beta_{11} \\ \beta_{12} \\ \vdots \\ \beta_{kk} \end{bmatrix}$$

where n is the number of combinations of wind climate parameters used to create the response surface. The regression parameters β are given by Equation (5.10). [Toft et al., 2015]

$$\hat{\beta} = (\mathbf{X^T X})^{-1}\mathbf{X^T f} \tag{5.10}$$

5.6 Taylor series

The Taylor-series are also applied to create the response models and the accuracy of those models will be compared to the results from the Central Composite Design. The Taylor series have been applied to the individual wind speed bins. The response denoted f, for a given vector of wind climate parameters $\mathbf{U} = [u_1, u_2 ...., u_i ..., u_k]^T$ is approximated by Equation (5.11).

$$f(\mathbf{U_0}) + \sum_{i=1}^{k} \frac{\partial f(\mathbf{U_0})}{\partial u_i}(u_i - u_{0,i}) \tag{5.11}$$

where $U_0 = [u_{0,1}, u_{0,2}, ..., u_{0,i}, ... u_{0,k}]^T$ corresponds to the reference wind climate parameters given by the wind turbine class. The response is formulated using dimensionless codified variables $\mathbf{X} = [x_1, x_2, ..., x_i ..., x_k]^T$ given by Equation (5.12).

$$x_i = \frac{u_i - u_i^0}{\Delta u_i^0} \tag{5.12}$$

where u_i^0 corresponds to the centre value and Δu_i^0 corresponds to the step value for the individual wind climate parameters applied to create the response surface. The forward finite difference method has been applied to approximate the first order partial derivative by applying the vector $\mathbf{X_0} = [x_{0,1}, x_{0,2}, ..., x_{0,i}, ..., x_{0,k}]^T$ which corresponds to the reference wind climate parameters and $\Delta x_i = [0, 0, ..., \Delta x_i, ..., 0]^T$ the response can be approximated by Equation (5.13).

$$f(\mathbf{X}) = f(\mathbf{x_0}) + \sum_{i=1}^{k} \frac{\partial \mathbf{f}}{\partial x_i}(x_i - x_{0,i}) + \sum_{i=1}^{k}\sum_{j=1}^{k} \frac{\partial \mathbf{f}}{\partial x_i \partial x_j}(x_i - x_{0,i})(x_j - x_{0,j}) \tag{5.13}$$

The forward finite difference is estimated based on the reference point $x_{0,i}$ and the two closest $x_i^{'}s$ using linear interpolation/extrapolation to determine the $f(\mathbf{x_0} + \mathbf{\Delta x_i})$. This approach improves the accuracy of the methodology, especially for nonlinear responses. [Toft et al., 2015].

The response models have been established from a reference points for climate parameters turbulence intensity and wind shear. This is done since the response models established from the Central Composite Design showed similar behaviour and also based on the plots of the response as a function of wind shear and turbulence intensity. The response models will be compared with simulations at the site by bootstrapping. On upcoming pages response models established with the Taylor-series are shown for certain wind speeds for specific components. The response models are established for DLC 1.2 and for DLC 1.3.

The response surface have been created for both DLC 1.2 and 1.3.

The figure on the left are the simulated response,the figure in the middle are the response established with Central Composite design and the the figures on the right are established with the Taylor-series.

5.6.1 Response surfaces - DLC 1.2

In this report it have been chosen to only show the load response surfaces and load response models for the components RootMyb (Flapwise bending moment) and TwrBSMyt (Tower bottom for-aft bending moment) for mean wind speed 5, 12 and 24 m/s. The rest of the response surfaces and response models are in Appendix B

The response surface for DLC 1.2 can be seen in the Figures below. The red mark on the models marks the reference points applied to create the response models.

DLC 1.2

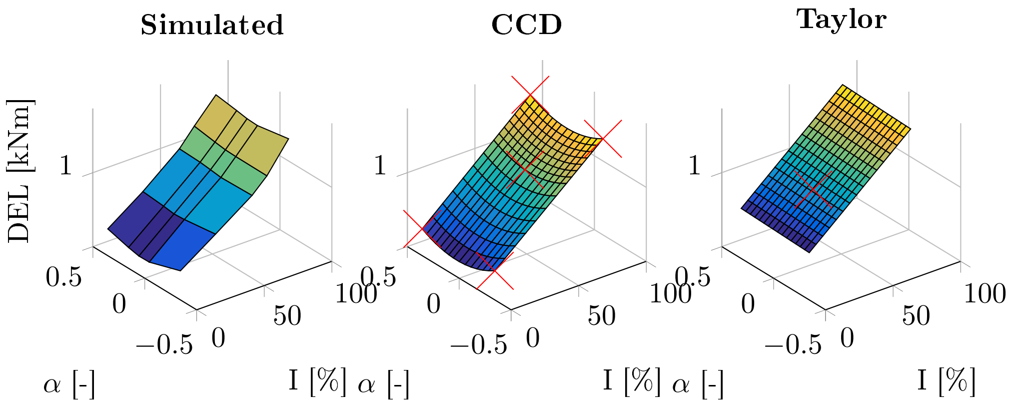

Figure 5.3: Flapwise bending moment 5 m/s.

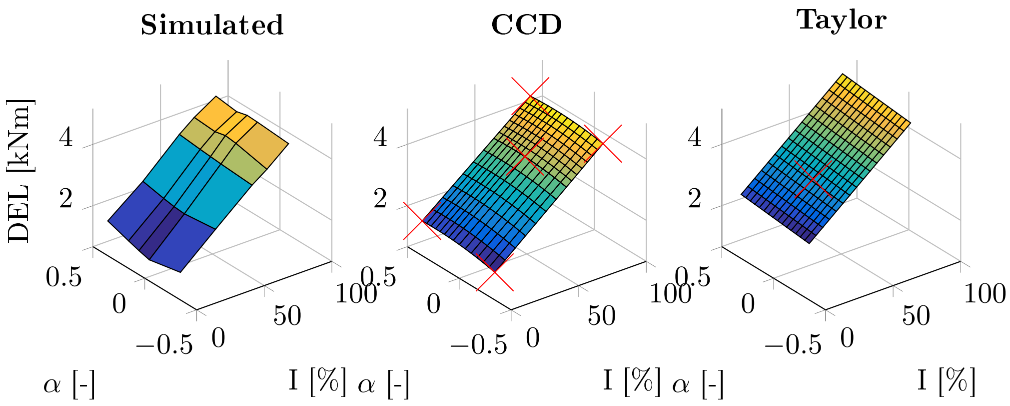

Figure 5.4: Flapwise bending moment 12 m/s.

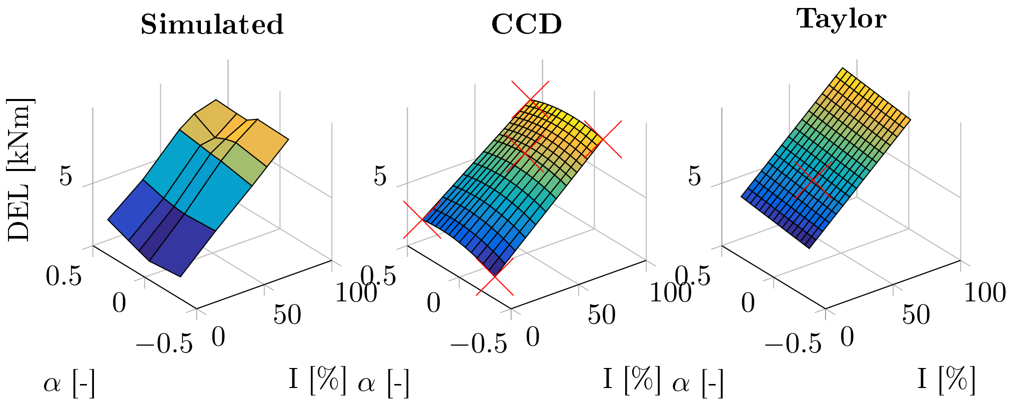

Figure 5.5: Flapwise bending moment 24 m/s.

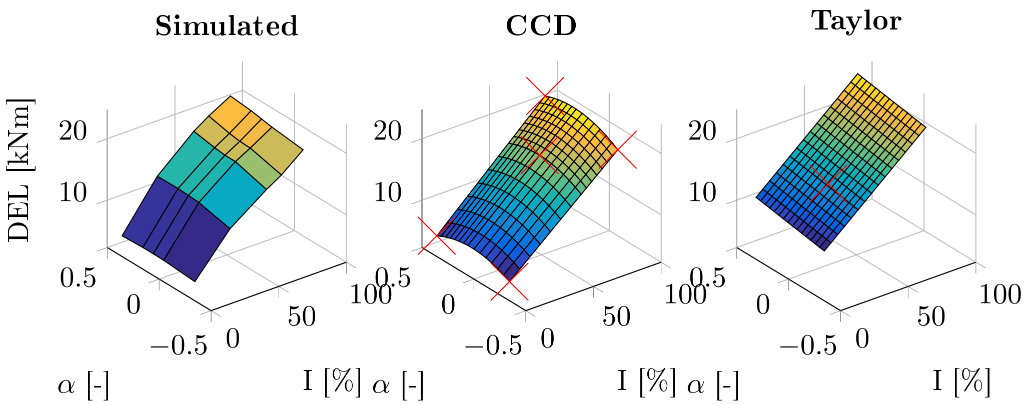

Figure 5.6: Tower bottom for-aft bending moment 5 m/s.

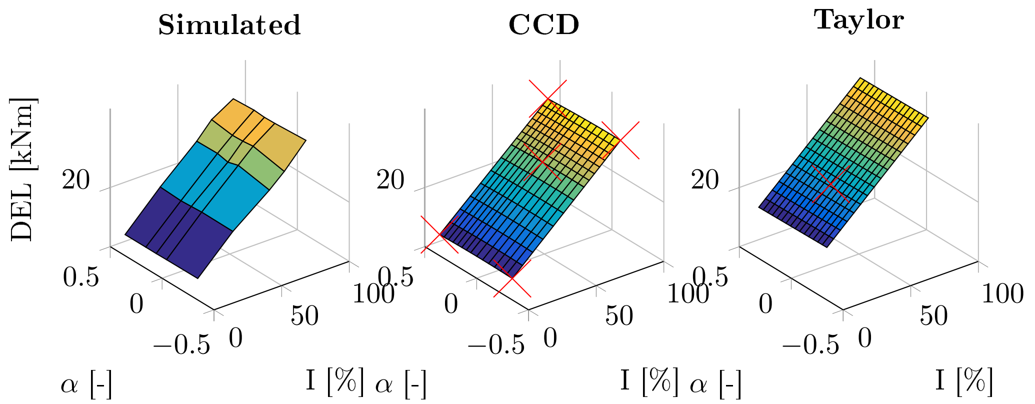

Figure 5.7: Tower bottom for-aft bending moment 12 m/s.

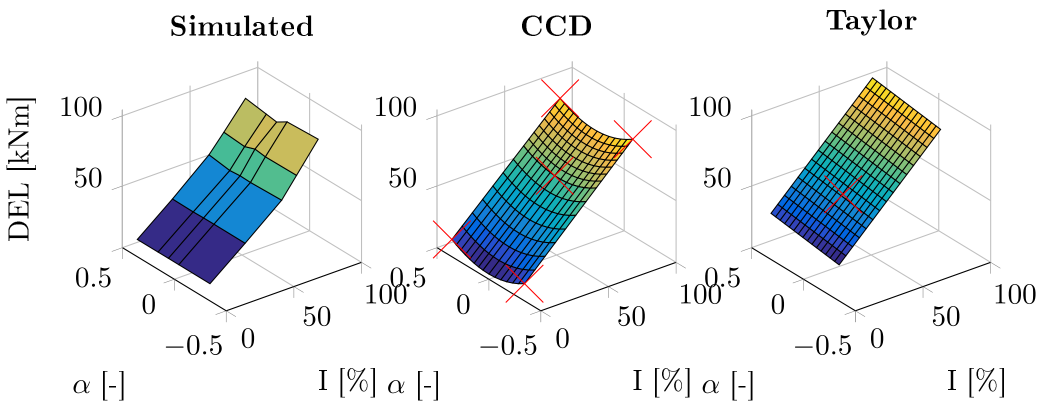

Figure 5.8: Tower bottom for-aft bending moment 24 m/s.

Comparing the above figures it is noticed that the response models established with the CCD follows the same trend as the simulated response surfaces. Analysing the simulated response surface it is seen that the trend of the response surface follows a second order polynomial shape as a function of wind shear and the CCD models follow a similar trend as a function of wind shear.

Some of the response surfaces show some discontinues in the surface, see Figure 5.5. This discontinuity might be due to the simulation has been initiated with high turbulence and high wind shear plus high wind speed and the control system of the wind turbine might have pitched the blades so the response suddenly decreases. Or there might have been some errors in these simulations. In general the response models from the Taylor-series predicts higher response in comparison to the simulated response surface and the CCD method. The turbulence intensity has a higher influence on the response compared the wind shear.

The response models for DLC 1.3 are presented below. The red mark on the response surface marks the reference point applied to create the response models. The same mean wind speed and components has been chosen for DLC 1.3 as it is then easier to compare the response surfaces with DLC 1.2.

DLC 1.3

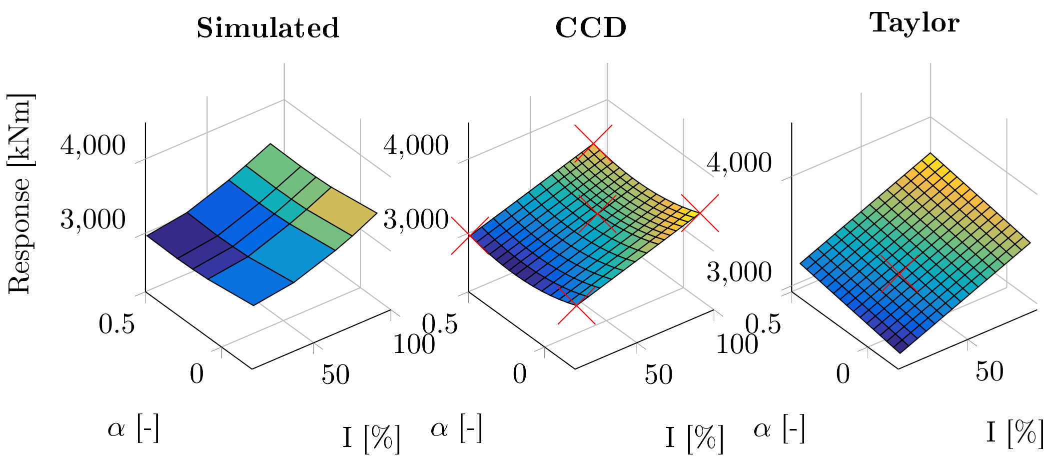

Figure 5.9: Flapwise bending moment 5 m/s.

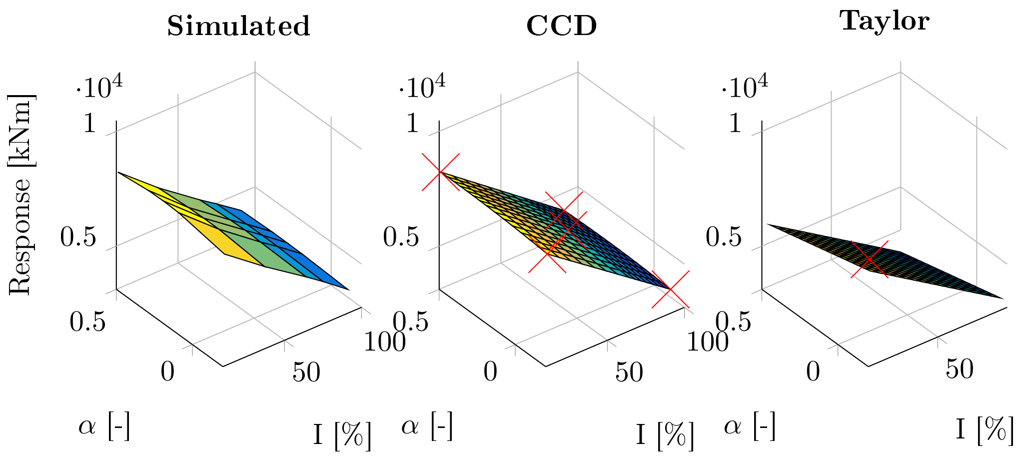

Figure 5.10: Flapwise bending moment 12 m/s.

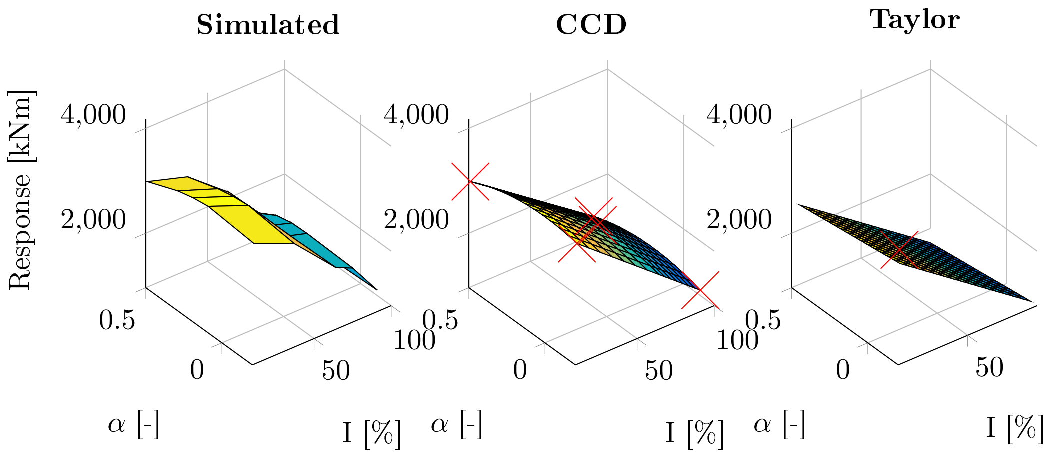

Figure 5.11: Flapwise bending moment 24 m/s.

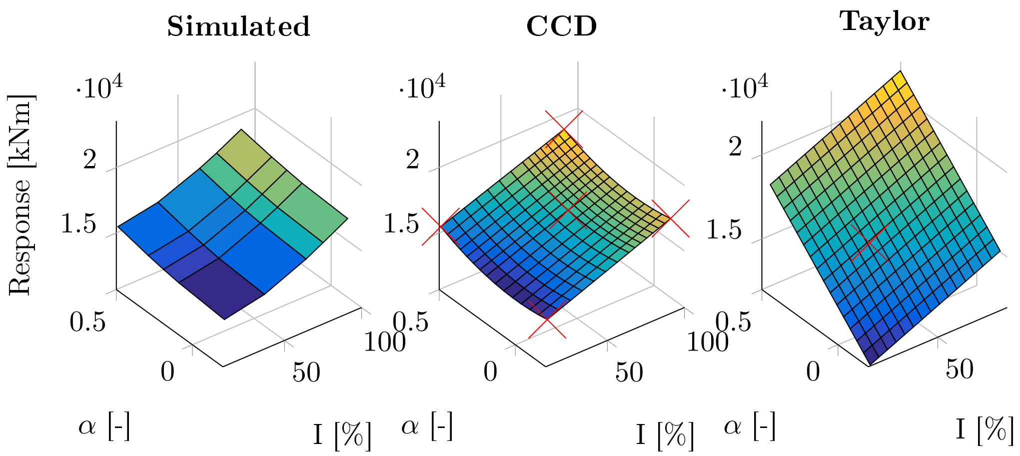

Figure 5.12: Tower bottom for-aft bending moment 5 m/s.

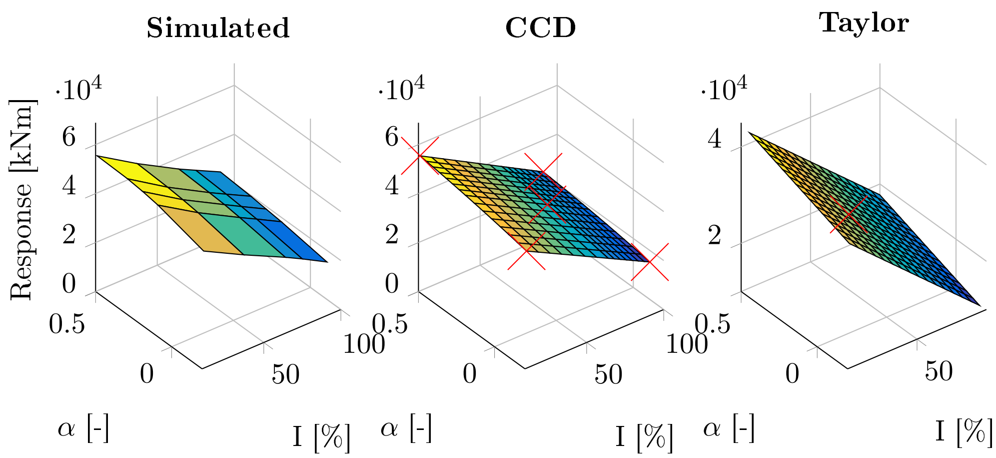

Figure 5.13: Tower bottom for-aft bending moment 12 m/s.

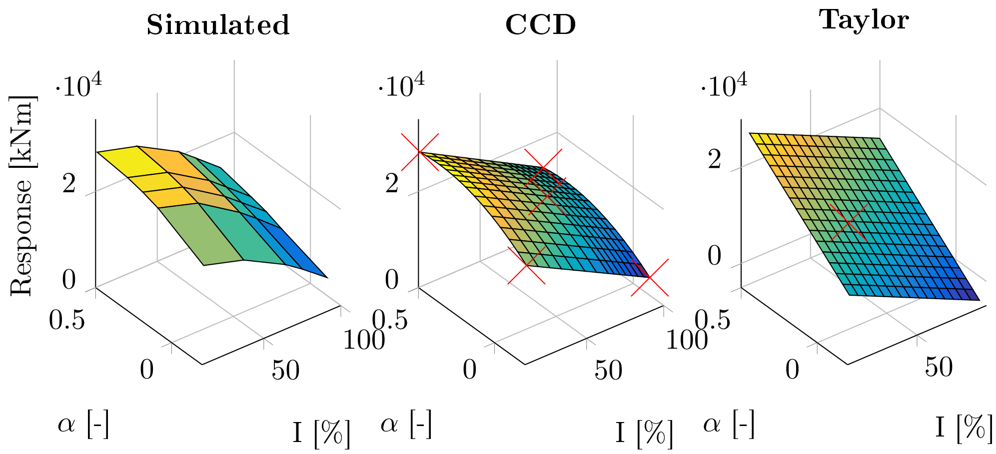

Figure 5.14: Tower bottom for-aft bending moment 24 m/s.

Similar to DLC 1.2 the turbulence intensity has the larger influence on the response compared to the wind shear. For both components at mean wind speeds of 12 and 24 m/s the response surface and response models change behaviour. At these wind speeds the loads decreases with increasing turbulence intensity. This might be due to the control system pitching the blades at these wind speeds. It has been verified that the turbine is not shutting down because of the high turbulence and high wind speed by analysing the power output at 24 m/s with a turbulence intensity at 91 %, see figure A.13. Similar to DLC 1.2 the response surface and response models established with CCD follows a curve shape or linear for the turbulence intensity and second order behaviour for the wind shear.

A second load sweep have been simulated. In this load sweep the turbulence intensity have been combined with the air density. Similar to the previous analyse the simulated response, regression models for CCD and Taylor-series are shown below for both DLC 1.2 and DLC 1.3.

For this analysis it has been chosen only to show the response surface and response models for component flapwise bending moment at mean wind speed 5, 12 and 24 m/s. The other models are in Appendix B.

DLC 1.2

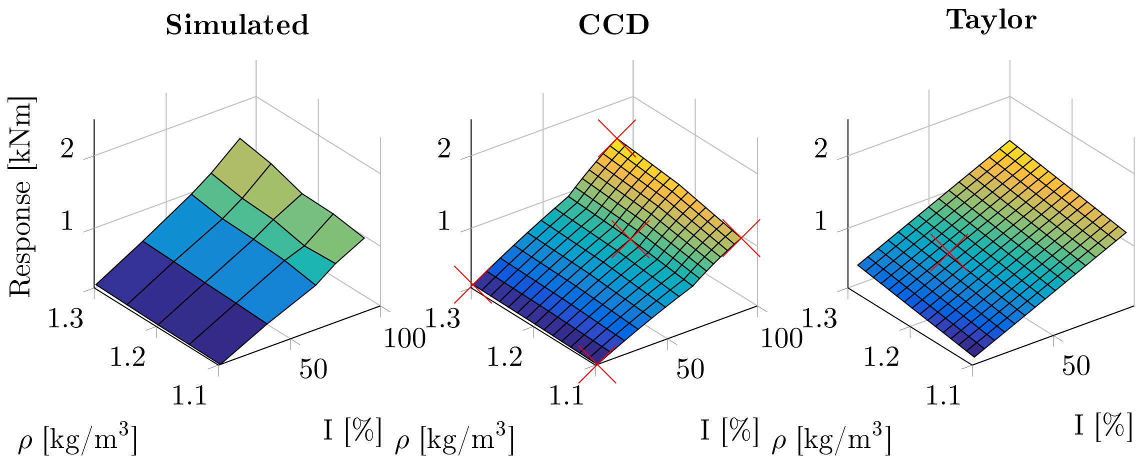

Figure 5.15: Flapwise bending moment 5 m/s.

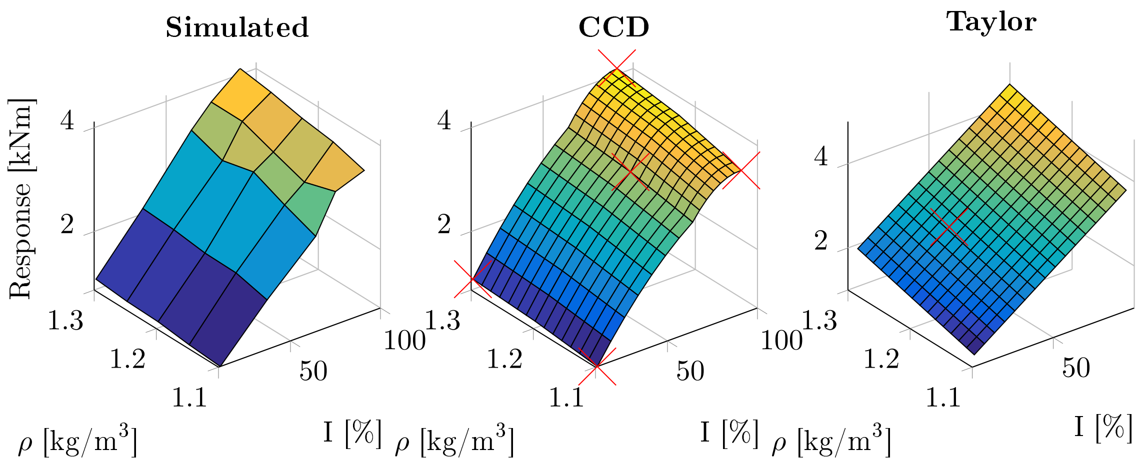

Figure 5.16: Flapwise bending moment 12 m/s.

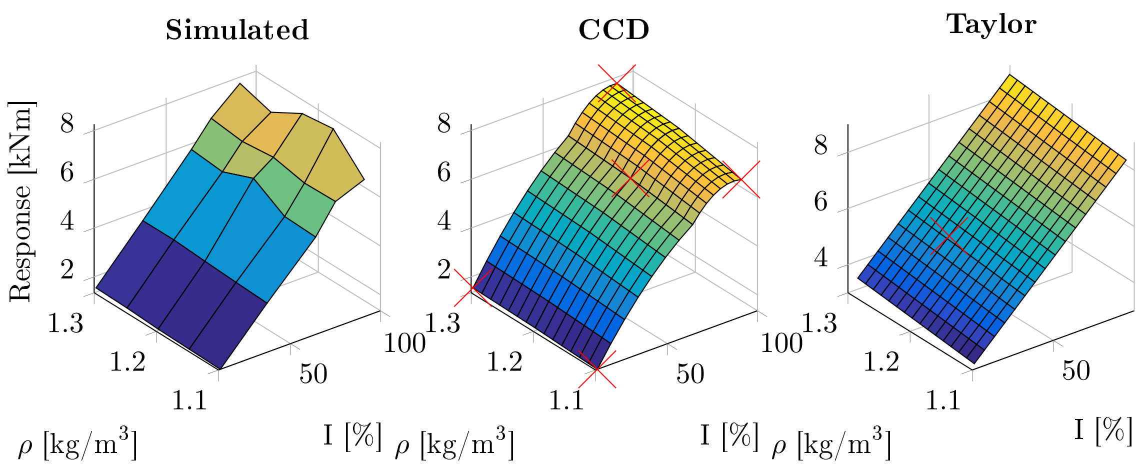

Figure 5.17: Flapwise bending moment 24 m/s.

Analysing the response surface it is seen that for mean wind speeds at 12, and 24 m/s there are some discontinuities at high turbulences, see Figure 5.16 and Figure 5.17 similar to Figure 5.5. This might be due to some errors in the simulations because of the high turbulence as input.

Similar to the first load sweep the regression models for the CCD-method are quite similar to the simulated response. In general the CCD-models behaves linearly as a function of the air density and a parabolic as function of the turbulence intensity. Regarding the Taylor-series it is seen that they are quite similar to the CCD-models although these models do not take the curve shape into account.

5.7 Loadsweeps with three climate parameters

In this section the response for three different climate parameters are presented in tables. The considered load sweeps can be seen in Table 5.1 (p. 28). The response presented below are determined with the CCD method for DLC 1.2 and 1.3 in Table 5.9 and Table 5.10.

For this analysis only the response from the CCD-method have been applied since it was concluded in the previous sections that the Taylor-series is not a sufficient method to establish a response model.

Table 5.9: Response. Flapwise bending moment DLC 1.2. Mean wind speed 5 m/s.

Turbulence intensity [%]	Wind shear [-]	Air density kg/m^3	Response [kNm]
11	0.2	1.225	2368.34
64	0.2	1.225	8256.16
91	0.2	1.225	14143.97
11	-0.2	1.225	2935.90
11	0.2	1.225	2368.34
11	0.5	1.225	2808.17
11	0.2	1.1	1881.87
11	0.2	1.225	10379.23
11	0.2	1.3	14708.07

It can be concluded from Table 5.9 the turbulence intensity has a large influence on the response when the turbulence intensity is increasing as expected from previous sections. The wind shear has a minor effect, but the air density has a large influence too which is unexpected from previous studies.

Table 5.10: Response. Flapwise bending moment DLC 1.3. Mean wind speed 5 m/s.

Turbulence intensity [%]	Wind shear	Air density	Response [kNm]
11	0.2	1.225	3400.29
64	0.2	1.225	2620.66
91	0.2	1.225	1841.03
11	-0.2	1.225	2938.67
11	0.2	1.225	3152.29
11	0.5	1.225	3333.46
11	0.2	1.1	2687.77
11	0.2	1.225	2940.13
11	0.2	1.3	3068.69

For this DLC the air density has not a large influence on the response compared to DLC 1.2 even though the same simulations are used for both design load cases.

Below are the response surfaces and response models shown for flapwise bending moment of mean wind speed 5, 12 and 24 m/s. The air density is held constant so it is possible to plot the figures and conclude these response surfaces and models are similar to Figure 5.3, Figure 5.4 and Figure 5.5.

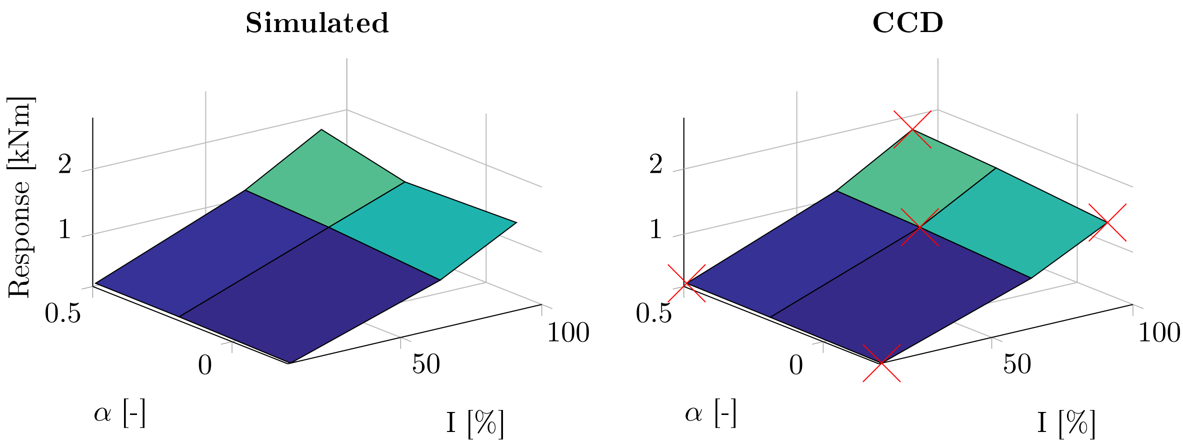

Figure 5.18: Flapwise bending moment 5 m/s. Air density 1.225 kg/m^3

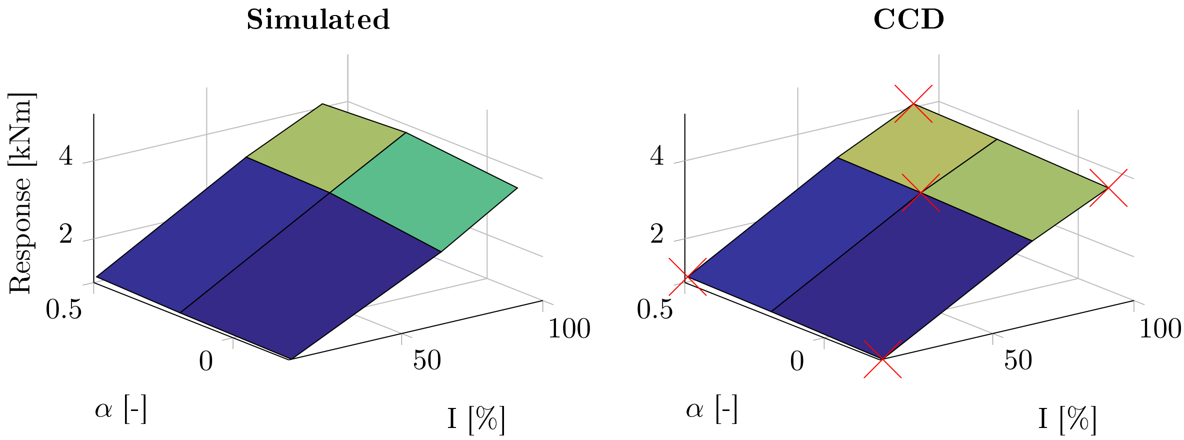

Figure 5.19: Flapwise bending moment 12 m/s. Air density 1.225 kg/m^3

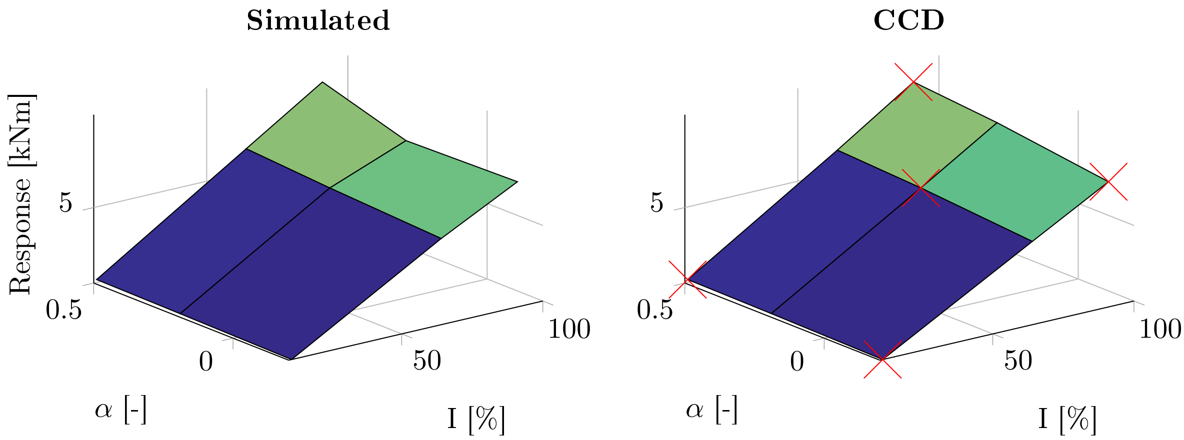

Figure 5.20: Flapwise bending moment 24 m/s. Air density 1.225 kg/m^3

Comparing the above figures with previous studies it can be concluded that they are similar even though they are established from different simulations. The response for other components and different mean wind speeds are in Appendix B.

Chapter 6

Benchmark

The purpose of this chapter is to benchmark, the DTU 10 MW turbine against the NREL 5 MW turbine. This is DCL 1.2 which addresses the issue of fatigue problem, in wind turbines. The components considered are presented in Table 2.4 (p. 10). 15 different simulations were made for each of the mean wind speed and the mean value of these simulations was used to generate these surface graphs.

FAST simulations done for the DTU 10 MW turbine has shown some issues, like e.g. when the simulation are running above rated wind speed the control system shuts the turbine down, and no usable results are generated. Therefore, the initial rotor speed has to be adjusted dependent on the 10-minute mean wind speed (see Table 6.1).

Table 6.1: Inital rotor speed

Wind speed [m/s]	Rotor [RPM]
5:11	9.6
12:23	5
24:25	3

The first four comparisons in the following section consider the impact of the wind shear coeffient dependent on the 10-minute mean wind speed and the resulting DEL. The variation for shear coefficient isvaried between -0.5 and 0.5 with 0.1 steps and the turbulence is set as a constant equal to 16 % in FAST and air density is set equal to 1.225 kg/m^3.

6.1 Wind shear variation

On the left side the NREL 5 MW turbine is illustrated and on the right side the DTU 10 MW turbine.

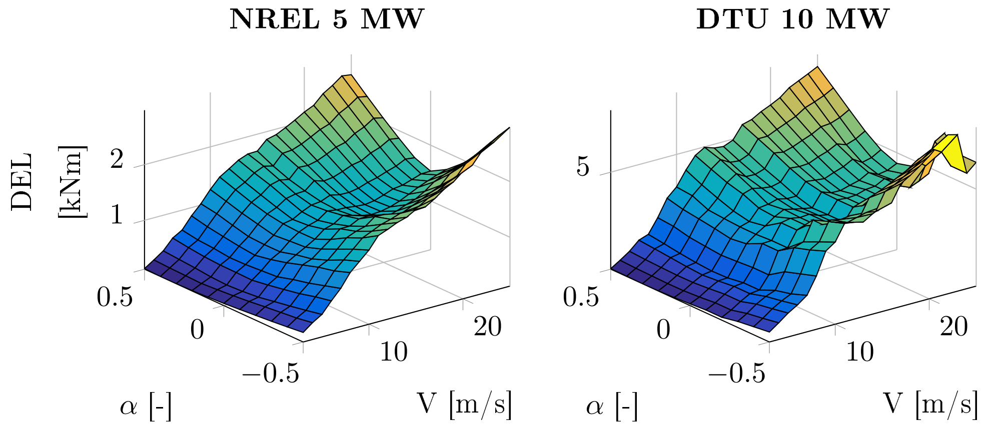

Figure 6.1: RootMyb1, flapwise bending moment.

Figure 6.1 shows a good similarity between the NREL 5 MW and the DTU 10 MW turbines. Though there are some inconsistenies in the high wind speed and negative wind shear range for the DTU 10 MW turbine.

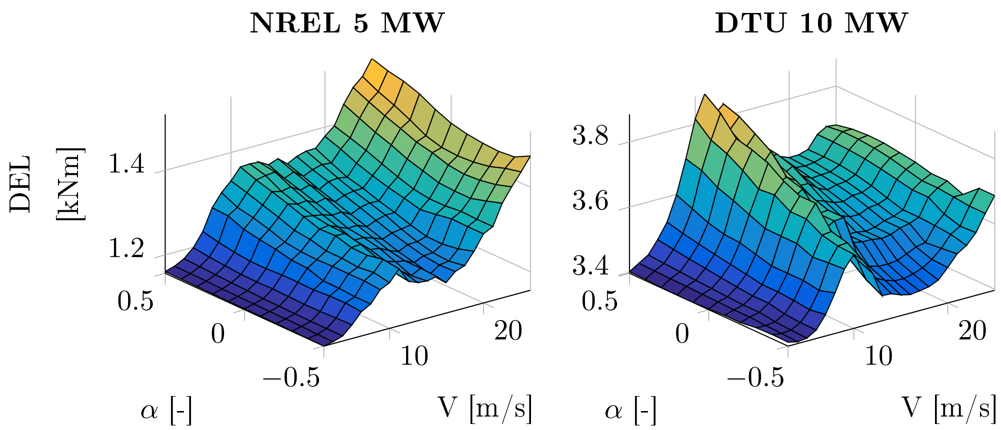

Figure 6.2: RootMxb1, edgewise bending moment.

The RootMxb1, Figure 6.2 both of the graphs show a growing response up to rated wind speed while the NREL 5 MW goes down and increases again, but the DTU 10 MW mostly goes down after rated wind speed.

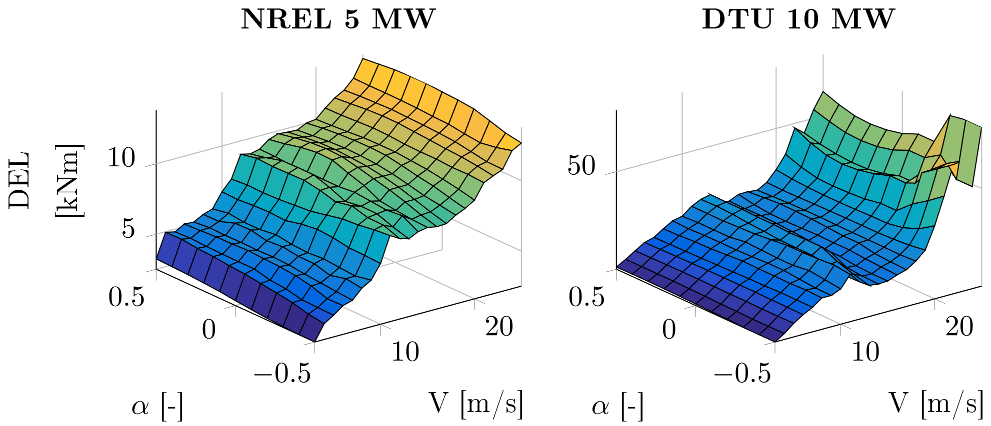

Figure 6.3: TwrBsMyt, tower for-aft moment.

The difference between the TwrBsMyt, Figure 6.3, while the NREL 5 MW increases almost linearly with the wind speed for each og the shear values. The DTU 10 MW does not show this trend it grows to rated wind speed and then declines and rises almost exponentially to 25 m/s.

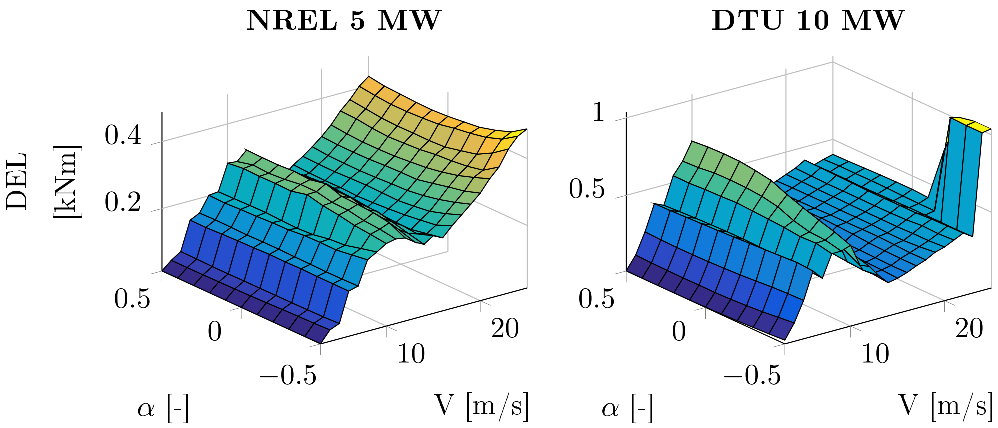

Figure 6.4: LSSGagMxa, low speed shaft torque.

The LSSGagMxa component, Figure 6.4 for NREL 5 MW turbine shows a growing trend to rated wind speed and declines a bit then increases again when increasing the 10-minute mean wind speed, while the DTU 10 MW does the same up to rated wind speed but however the response becomes almost constant up to 25 m/s. The issue with the high wind speed and low wind shear values is most apparent in this graph. This problem might be caused by some of the initial values for the numerical calculations are violated as these are in reality extreme values.

6.2 Turbulence intensity variation

For the turbulence intensity, the simulations are made from the interval 0:30 % and the shear coefficient equal to 0.2 and the same air density at 1.225 kg/m^3.

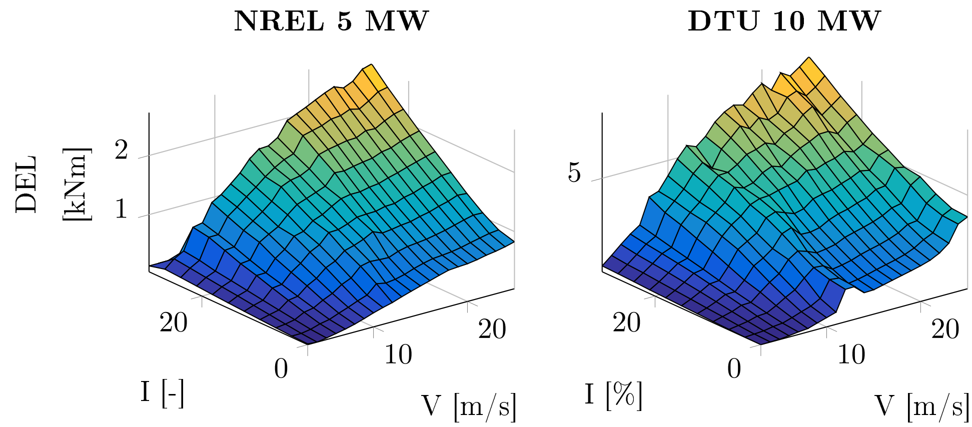

Figure 6.5: RootMyb1, flapwise bending moment.

The RootMyb1, which is shown in Figure 6.5, shows good relations between the two turbines. They show the same trend and, as expected, the DTU 10 MW shows higher response values.

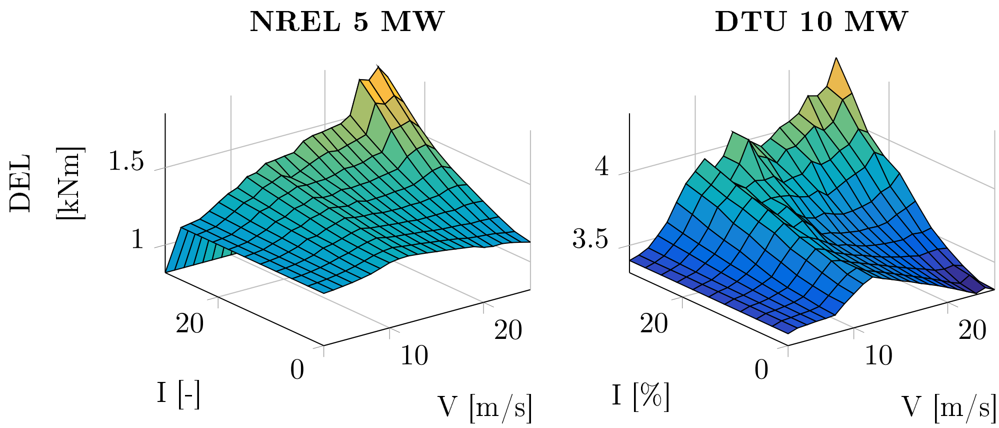

Figure 6.6: RootMxb1, edgewise bending moment.

The RootMxb1, presented in Figure 6.6, show that there have been some issues with the NREL 5 MW simulations for turbulence intensity of 30 %. This could be because the NREL 5 MW simulations make the turbine shut down and results in the low response values. But the overall trend between the two graphs seems to match.

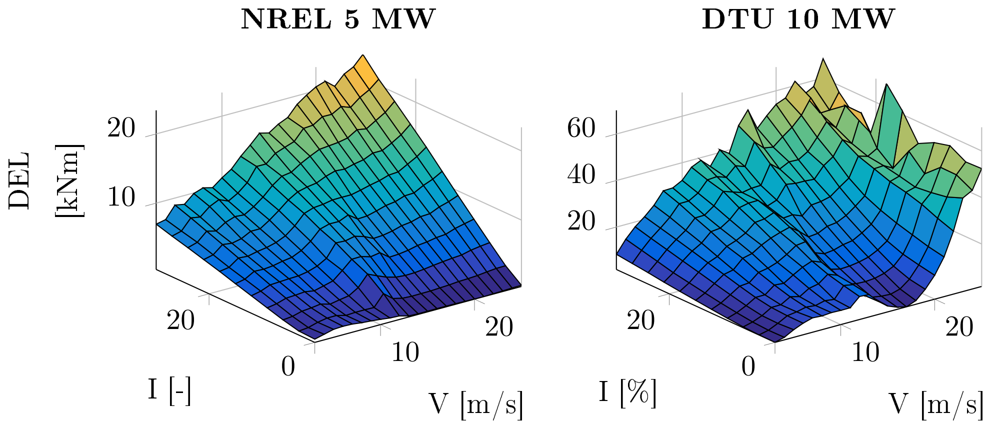

Figure 6.7: TwrBsMyt, tower for-aft moment.

TwrBsMyt, shown in Figure 6.7 gives a non-linear response behaviour of the DTU 10 MW turbine simulations for high wind speed values. This could be caused by the influence of the turbine being shut down as this is in the extreme high wind speed domain.

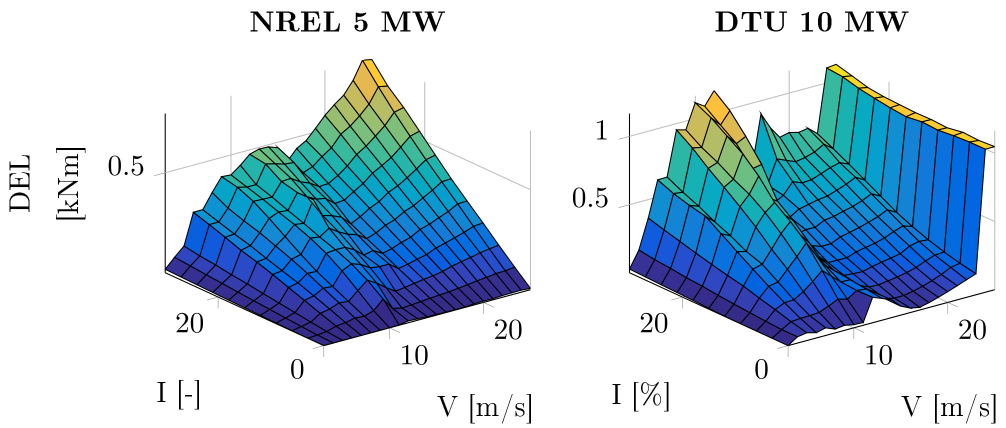

Figure 6.8: LSSGagMxa, low speed shaft torque.

The LSSGagMxa presented in Figure 6.8 shows inconsistency between the NREL 5 MW and the DTU 10 MW turbines. This might be caused by difference in control algorithms between the two models. However, at 25 m/s, responses are very odd. The responses seem to be too high in relation to previous mean wind speeds.

In general the DTU 10 MW plots are more rigid even though they have the same amount of seeds as the NREL 5 MW. This might be caused by the sensitivity of the DTU 10 MW model in FAST.

The RootMyb1 (flapwise bending moment) plots show for both wind turbine types, the same trend while the RootMxb1 (edgewise bending moment) differs a bit in the high wind speed region. The TwrBsMyt, grows quite regular with increasing wind speeds for the NREL 5 MW turbine while the tower bottom for-aft bending moment at the DTU 10 MW turbine first increases when moving to high wind speeds. it should be noted that the response difference for the tower between the two turbines is quite high.

Focusing on the plots with the turbulence variation, the trend for RootMyb and RootMxb, are quite similar for both turbines. At high wind speeds the TwrBsMyt response surface behave non-linear and shows high fluctuations in the responses. The LssGagMxa is the component that shows the strangest behaviour for the DTU 10 MW.

Chapter 7

10 MW Turbine Load Sweeps, DLC 1.2

This section is about simulations that were done for DTU 10 MW turbine and generated CCD models. The difference in these simulations from previous simulations is that, only the first six seeds are used to save time to simulate the data. The climate parameters and the load sweeps can be seen in Table 7.1. The reason for the change in turbulence intensity, is caused by the numerical instability of the model in FAST, when it was running for higher values of turbulence resulting in that the turbine went to shut down mode.

Table 7.1: Variation of the climate parameters.

Wind speed	5 12 24	[m/s]
Air density	1.100 1.225 1.300	[kg/m^3]
Turbulence intensity	11 20 30	[%]
Wind shear	-0.2 0.2 0.5	[-]

An example of a time series is shown in Figure 7.1. The problem when the turbulence was high as done for previous load sweeps the generated power was zero, and the responses for the components where useless was solved was solved by defining a new interval. Defining a new interval for the turbulence intensity as resulted in more useful responses.

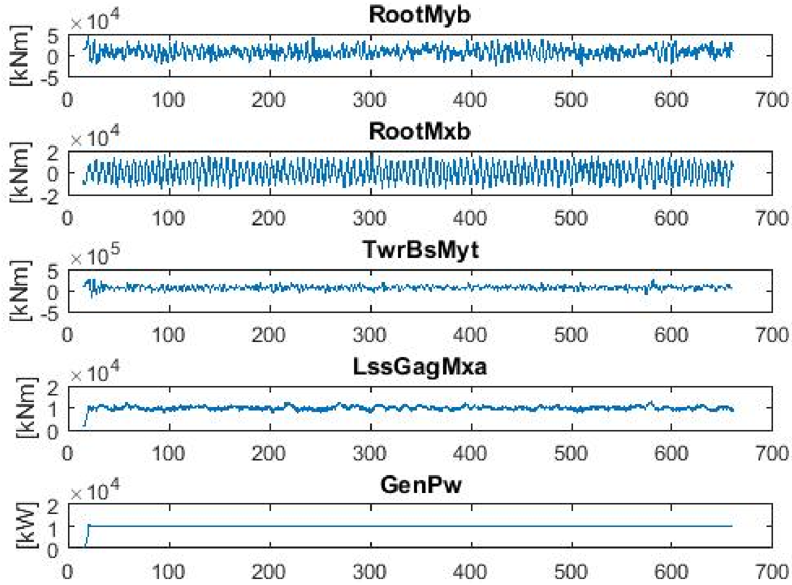

Figure 7.1: Time series, mean wind 24 m/s, turbulence intensity 30 % and ρ 1.300 kg/m^3.

From Figure 7.1, it can be seen that the generated power becomes constant after few seconds. The time series for the components also shows a reasonable fluctuations. Only few seeds resulted in turbine shut down. Shut down mainly occured at high wind speeds and high turbulence levels.

7.1 DTU 10 MW Load Sweeps

The simulations and models for RootMyb (flapwis bending moment) can be seen in the figures below. On the figures for CCD the red crosses note the point used from the simulations to generate the models. The figures for other components are in Appendix B.

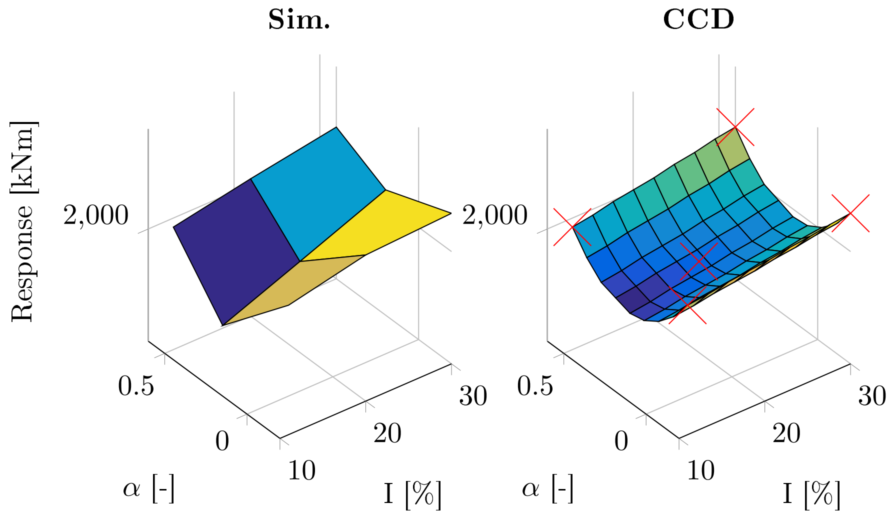

Figure 7.2: RootMyb1, 5 [m/s] ρ 1.100 [kg/m^3].

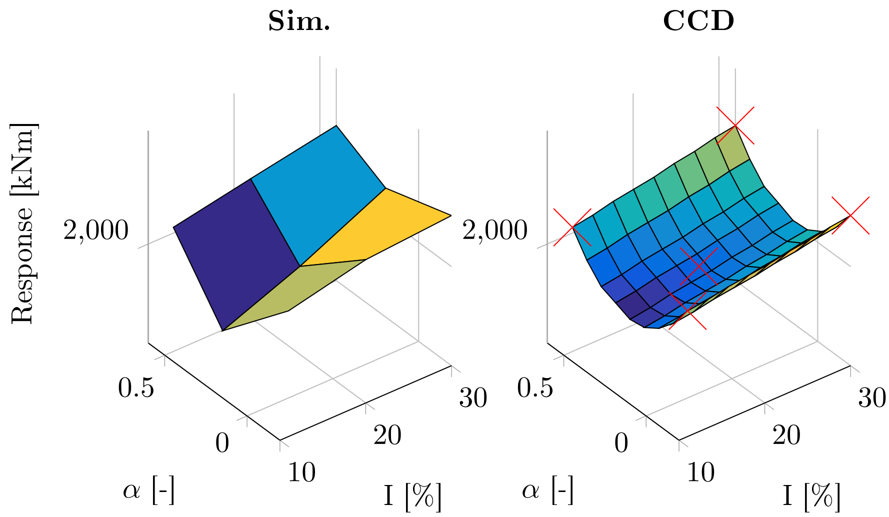

Figure 7.3: RootMyb1, 5 [m/s] ρ 1.225 [kg/m^3].

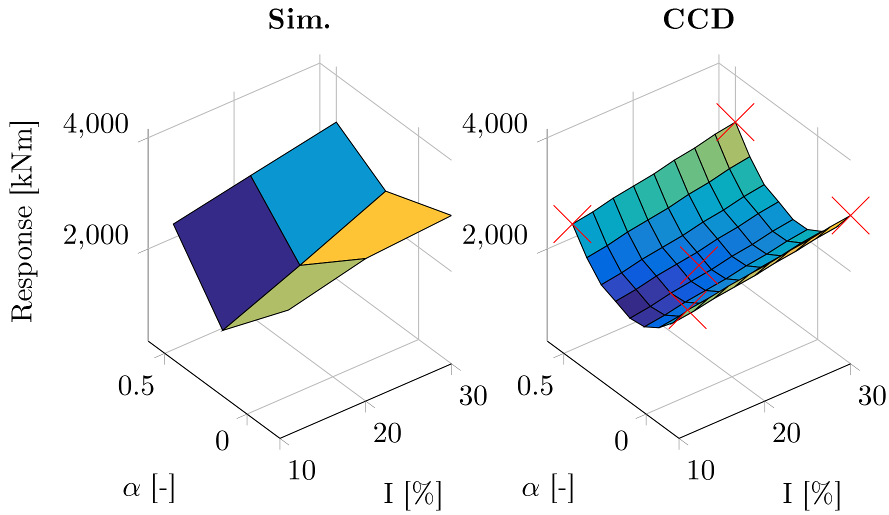

Figure 7.4: RootMyb1, 5 [m/s] ρ 1.300 [kg/m^3].

For the RootMyb the simulations and models show the same trend, the responses for the simulations are not varying much.

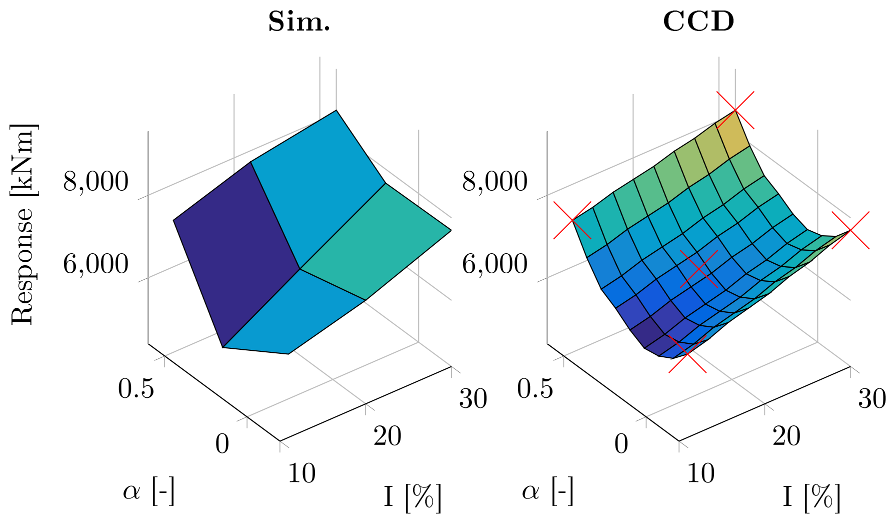

Figure 7.5: RootMyb1, 12 [m/s] ρ 1.100 [kg/m^3].

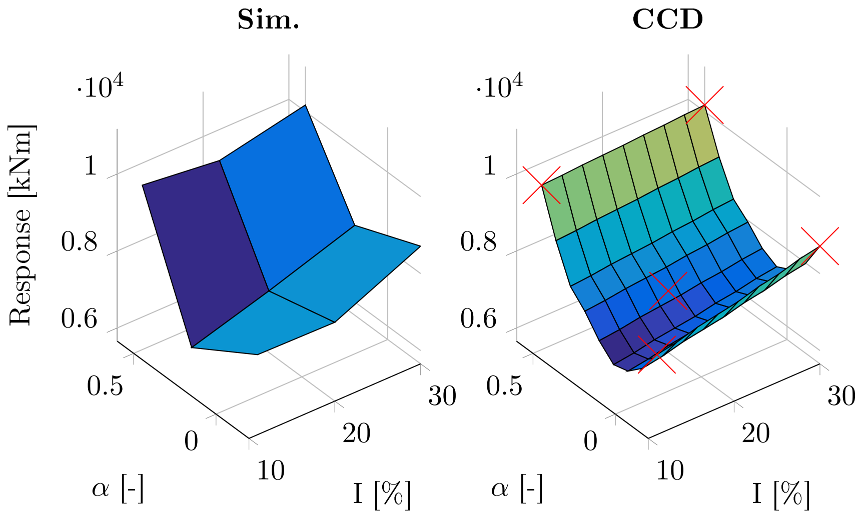

Figure 7.6: RootMyb1, 12 [m/s] ρ 1.225 [kg/m^3].

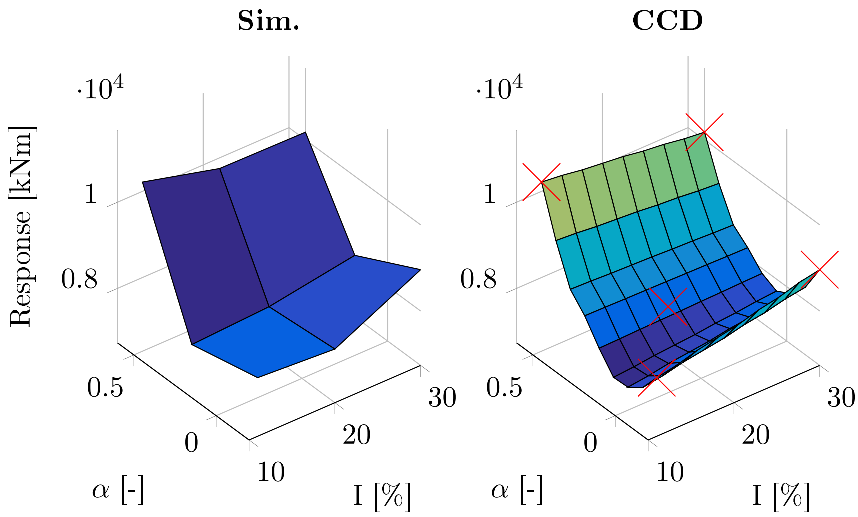

Figure 7.7: RootMyb1, 12 [m/s] ρ 1.300 [kg/m^3].

As the wind speed increases, the responses for the wind shear start to vary more and as the CCD model only uses the corners and center to generate the surface the actual responses for wind shear around 0.2 is fails to represent in the model for the outer values of the turbulence intensity.

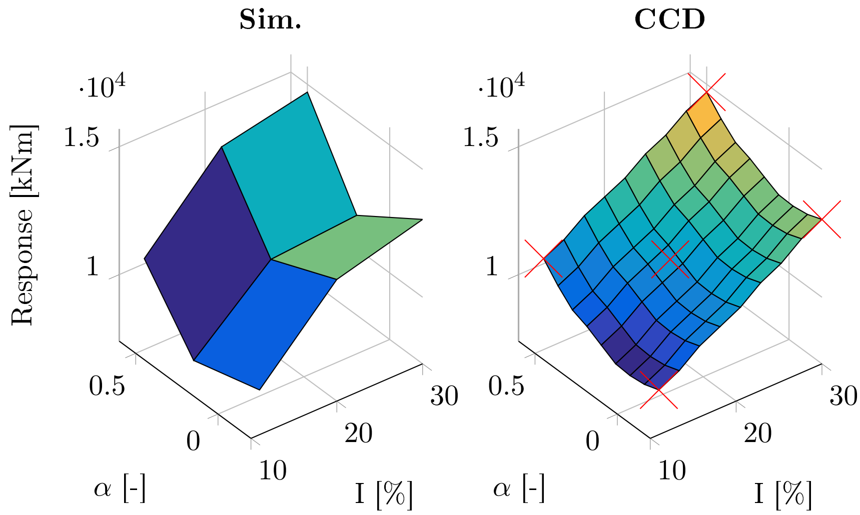

Figure 7.8: RootMyb1, 24 [m/s] ρ 1.100 [kg/m^3].

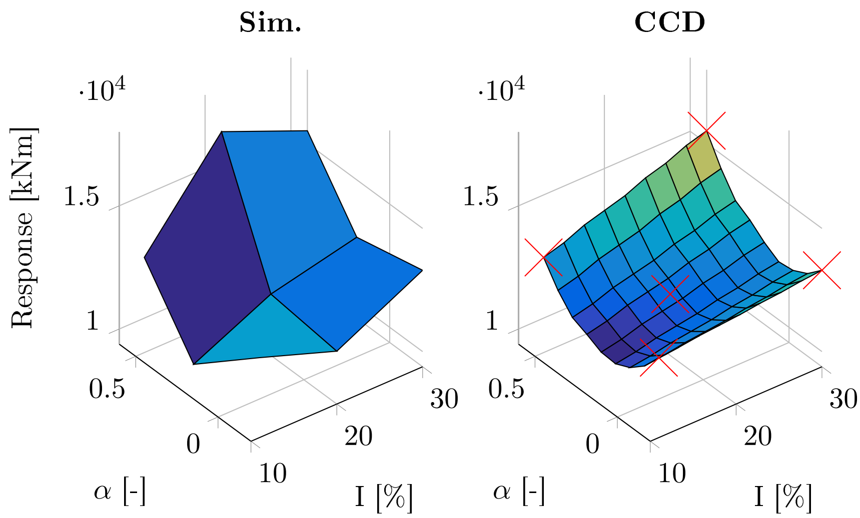

Figure 7.9: RootMyb1, 24 [m/s] ρ 1.225 [kg/m^3].

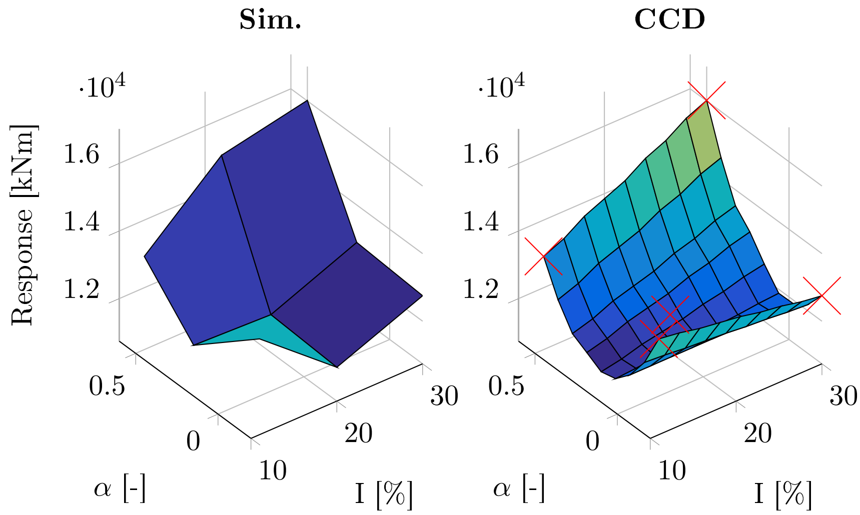

Figure 7.10: RootMyb1, 24 [m/s] ρ 1.300 [kg/m^3].

For 24 m/s the simulations start to show a much more non-linear trend between the reference points and the CCD model is not optimal to describe the behaviour of the turbine.

In general the CCD models can fairly follow the same trend presented in the simulated data and show the same response value for the models for wind speed 5 m/s, as these simulations show a linear surface graph which increases more or less linearly with the turbulence intensity and wind shear values. The problem persists with wind speeds of 12 and 24 m/s. There the simulations start to show a very non-linear trend, which the CCD models cannot estimate well. All the models can be found in Appendix B.

Chapter 8

Uncertainty analysis

The purpose of this chapter is to analyse the uncertainty of the climate parameters on the response models. In previous sections response models for the NREL 5 MW turbine and the DTU 10 MW turbine have been established of the Central Composite design method. The sensitivity analysis only concerns the response models established with the CCD-method because it was concluded in previous sections that the CCD-method fits the response from the simulations more precisely.

In order to asses the influence of the uncertainty of the climate parameters on the response models EMD have provided the project group with some data. In general the response surfaces are established for various response quantities Q and is given by Equation (8.1).

$$Q = X_\epsilon Q(\vec{V}, I, \alpha, \rho) \tag{8.1}$$

where:

$\vec{v}$	long-term mean wind speed at hub height [m/s]
X_ϵ	response model uncertainty assumed to be Lognormal distributed
	with mean value = 1 and coefficient of variation = $V_\epsilon[-]$

For DLC 1.2 it is assumed that:

- $\vec{v}$ is Rayleigh distributed with mean value = V_{ave} where $V_{ave} = 0.2V_{ref}$, given in Section 6.3.1.1 in IEC 61400-1ed.3. Values of V_{ref} for different wind classes are shown in Table 1 in IEC 61400-1ed.3. In general $\vec{v}$ can be assumed to be Weibull distributed with size parameter A and scale parameter k. If k = 2 then A = $\frac{2}{\sqrt{\pi}}V_{ave}$
- I is Lognormal distributed (IEC 61400-1 ed.3) with
  - mean value $\mu_1(\vec{v} = I_{15}(0.75\vec{V} + 3.8)$ (units in m/s)
  - standard deviation $\sigma_1 = I_{15} \cdot 1.4$ and
  - 90% quantile $I_{90} = I_{15}(0.75\vec{V} + 5.6)$ (units in m/s)
    where I_{15} is the reference turbulence intensity at 15 m/s

The resulting total lifetime fatigue damage is assumed to be proportional to e.g. a fatigue equivalent load obtained by assuming Q, in Equation (8.2) is the corresponding load for given $\vec{V}$, I, α and ρ in Equation (8.2).

$$
\begin{aligned}
Q_T(A,k,I_{15},\alpha,\rho) &= X_\epsilon \int_{V_{in}}^{V_{out}} Q\left(\vec{v},I = I_{15}\left(0.75\vec{V} + 5.6\right),\alpha,\rho\right) f_{\vec{v}}\left(\vec{v};A,k\right) d\vec{v} \\
Q_T(A,k,I_{15},\alpha,\rho) &= \sum_{i=1}^{n_y} Q\left(\vec{V}_i,I = I_{15}\left(0.75\vec{V}_i + 5.6)\right),\alpha,\rho\right) P_{\vec{v}}(\vec{v_i};A,k)
\end{aligned}
\tag{8.2}
$$

$P_{\vec{v}}\left(\vec{v_i};A,k\right)$ is the probability of wind speed $\vec{v_i}$ in bin no. i and n_v is number of bins. The 90% quantile is used for calculation of I.

For DLC 1.3 it is assumed that:

- I is obtained as the 50 year value according to IEC 61400-1 ed 3 with $I_{50}(\vec{v}) = cI_{15}\left(0.072\left(\frac{A}{c}+3\right)\left(\frac{V}{c}-4\right)+10\right)$, $c = 2$ (units in m/s)

The resulting 50 year load effect Q_{50} is obtained assuming that the load effect in Equation (8.1) is given in Equation (8.3).

$$
\begin{gathered}
Q_{50}(A,I_{15},\alpha,\rho) = X_\epsilon max Q(\vec{V},I_50(\vec{V},I_50),\alpha,\rho) \\
\vec{V} \in [V_{in},V_{out}]
\end{gathered}
\tag{8.3}
$$

The maximization of Equation (8.3) can be solved approximately by considering only the rated wind speed and the cut-out wind speed. The climate parameters are subjected to a uncertainty that is assumed to be expressed by the corresponding coefficient of variations, see Table 8.1. In most cases A and k are correlated with correlation coefficient ρ_A,k.

Table 8.1: Coefficient of variations of the climate parameters.

V_A for A
V_k for k
V_I for I
V_α for α
V_ρ for ρ

Based on a first order linearisation of the load effect the resulting uncertainty of the response

Q can be expressed by the coefficient of variation, see Equation (8.4).

$$V_{Q_x} = (V_\epsilon^2 + ((\frac{1}{Q_{xm}})^2 \left(\frac{dQ_x}{dA}\mu_A V_A\right)^2 + \left(\frac{dQ_x}{dk}\mu_k V_k\right)^2 + 2\left(\frac{dQ_x}{dA}\frac{dQ_x}{dk}\rho_{A,k}\mu_A\mu_k V_A V_k\right) + \left(\frac{dQ_x}{dI_{15}}\mu_{I_{15}} V_{I_{15}}\right)^2 + \left(\frac{dQ_x}{d\alpha}\mu_\alpha V_\alpha\right)^2 + \left(\frac{dQ_x}{d\rho}\mu_\rho V_\rho\right)^2))^{(1/2)} \tag{8.4}$$

where $\frac{dQ_x}{dA}$,.... are the derivatives of Q_x with respect to the climate parameters, which can be obtained by numerical differentiation using the response surfaces. Q_{xm} represents the response obtained using base values of the climate parameters.

Mean values of the climate parameters used for the calculation are given in Table 8.2.

Table 8.2: Mean values of climate parameters.

$\mu_{I_{15}}$ [m/s]	0.16
μ_α [-]	0.2
μ_ρ [kg/m^3]	1.15
μ_A [m/s]	8.5
μ_k [-]	3

The derivatives of Q_x for DLC 1.2 can be seen in Table 8.3.

Table 8.3: Derivatives of Q_x with respect to the climate parameters. DLC 1.2. Flapwise bending moment.

CCD	$\frac{\partial Qx}{\partial I}$ 0.21	$\frac{\partial Qx}{\partial \alpha}$ 0.0006	$\frac{\partial Qx}{\partial \rho}$ 0.001	$\frac{\partial Qx}{\partial A}$ -0.0020	$\frac{\partial Qx}{\partial k}$ -0.0028

Representative values of uncertainties are listed in Table 8.4 and Table 8.5.

Table 8.4: Coefficient of variations of the climate parameters and responses. DLC 1.2. Flapwise bending moment.

COV/Parameters	Case 1	Case 2	Case 3	Case 4	Case 5	Case 6
V_{I15} 10-30%	**10**	**30**	20	20	20	20
V_α 10-30%	20	20	**10**	**30**	20	20
V_ρ 5-10%	7.5	7.5	7.5	7.5	**5**	**10**
V_A 5-10%	7.5	7.5	7.5	7.5	7.5	7.5
V_k 1-5 %	2.5	2.5	2.5	2.5	2.5	2.5
$\rho_{a,k}$ 0.5-1.0	0.75	0.75	0.75	0.75	0.75	0.75
$V_{\sigma CCD}$	0.149194	0.421458	0.283762	0.283766	0.283764	0.283764

$V_{\sigma CCD}$ is the coefficient of variation of flapwise bending moment accounting for the uncertainties related to the climate parameters (obtained at a site assessment). Analysing the variance in Table 8.4 it is observed changing the coefficient of variation of the turbulence intensity has larger influence compared to effect of changing the COV of wind shear or air density which is close to none.

Table 8.5: Coefficient of variations of the climate parameters and responses. DLC 1.2. Flapwise bending moment.

COV/Parameters	Case 7	Case 8	Case 9	Case 10	Case 11	Case 12
V_{I15} 10-30%	20	20	20	20	20	20
V_{α} 10-30%	20	20	20	20	20	20
V_{ρ} 5-10%	7.5	7.5	7.5	7.5	7.5	7.5
V_A 5-10%	**5**	**10**	7.5	7.5	7.5	7.5
V_k 1-5 %	2.5	2.5	**1**	**5**	2.5	2.5
$\rho_{a,k}$ 0.5-1.0	0.75	0.75	0.75	0.75	**0.5**	**1.0**
$V_{\sigma CCD}$	0.282563	0.285165	0.283072	0.284441	0.280823	0.291748

Analysing the variance in Table 8.5 of the response it is seen that changing the COV of the size parameter A and the scale parameter in the Weibull distribution do have an effect on the result. The correlation coefficient between A and k increases as well. It was unexpected that the Weibull parameters are more sensitive than the wind shear and air density for this DLC.

The derivatives of Q_x for DLC 1.3 can be seen in Table 8.6

Table 8.6: Derivatives of Q_x with respect to the climate parameters.. DLC 1.3. Flapwise bending moment.

CCD	$\frac{\partial Qx}{\partial I}$ -0.33	$\frac{\partial Qx}{\partial \alpha}$ -0.14	$\frac{\partial Qx}{\partial \rho}$ 0.03	$\frac{\partial Qx}{\partial A}$ 0.02

Similar analysis have been done with DLC 1.3 see Table 8.7 and Table 8.8

Table 8.7: Coefficient of variations of the climate parameters and responses. DLC 1.3. Flapwise bending moment.

COV/Parameters	Case 1	Case 2	Case 3	Case 4	Case 5	Case 6
V_{I15} 10-30%	**10**	**30**	20	20	20	20
V_{α} 10-30%	20	20	**10**	**30**	20	20
V_{ρ} 5-10%	7.5	7.5	7.5	7.5	**5**	**10**
V_A 5-10%	7.5	7.5	7.5	7.5	7.5	7.5
V_k 1-5 %	2.5	2.5	2.5	2.5	2.5	2.5
$\rho_{a,k}$ 0.5-1.0	0.75	0.75	0.75	0.75	0.75	0.75
$V_{\sigma CCD}$	0.008113	0.008116	0.008101	0.008136	0.008114	0.008115

It is seen in Table 8.7 that opposite to DLC 1.2 increasing the coefficient of variation of the reference turbulence increases has no effect. However changing the coefficient of variation for the wind shear by the same amount has larger influences on the results, but for the air density it has no influence.

Table 8.8: Coefficient of variations of the climate parameters responses. DLC 1.3. Flapwise bending moment.

COV/Parameters	Case 7	Case 8	Case 9	Case 10	Case 11	Case 12
V_{I15} 10-30%	20	20	20	20	20	20
V_{α} 10-30%	20	20	20	20	20	20
V_{ρ} 5-10%	7.5	7.5	7.5	7.5	7.5	7.5
V_A 5-10%	**5**	**10**	7.5	7.5	7.5	7.5
V_k 1-5 %	2.5	2.5	**1**	**5**	2.5	2.5
$\rho_{a,k}$ 0.5-1.0	0.75	0.75	0.75	0.75	**0.5**	**1.0**
$V_{\sigma CCD}$	0.008113	0.008117	0.008114	0.008114	0.008114	0.008114

Analysing the results in Table 8.8 of the response, it is seen that changing the COV of the size parameter A has an influence on the results compared to the scale parameter k in the Weibull distribution. The correlation coefficient between A and k has no effect. This conclusion is opposite compared to the conclusion for DLC 1.2.

The sensitivity of the differently climate parameters are depending which DLC is analysed. From the results it is obvious that the turbulence intensity is the most sensitive climate parameter for DLC 1.2 which is reasonable based on the studies of the response models, however for DLC 1.3 the wind shear is more sensitive which is unexpected.

Chapter 9

Conclusion

The turbulence intensity from the data given from EMD A/S compared against the IEC 64100 ed3. standard (IEC), is rather different. For the given data the 90 % quantile is lower than the expected values from IEC for the Normal Turbulence Model (NTM) class A. The Extreme Turbulence Model (ETM) is lower than the 50 years values.

By estimating the turbulence intensity with more precision the simulations would result in more accurate data. As the IEC standard does not take into account wind direction the distribution of wind is fairly one sided, but analysing Figure 3.2 (p. 12) it can be seen that the wind speed varies coming from coast or land. The reduction of the wind speed can clearly be seen comparing these two figures. The statistical analysis shows that the IEC standard is conservative for a general site, but it is stated in IEC that it is possible to use site specific data, if data is provided.

A new version of IEC standard is presently under way, in this new version it is concluded that a Weibull distribution should be used to distribute the turbulence intensity. In the analysis where the Log-Normal and Weibull where compared on the data. It was concluded that the Weibull distribution was a better fit than the Log-Normal distribution, by fitting goodness, the difference nevertheless was minor.

Several analysis were done in FAST to verify the output, consisted of convergence of grid points, turbulence intensity and stabilisation. Changing the grid size resulted in lesser change in responses, but great increase in simulation time as seen in Table 4.2 (p. 20).It was decided to use 15x15 grid points using more than that would lead to more time consuming simulations but the increase in accuracy is minor. Some variation was found in the turbulence intensity where the input was not matched by the output, this was found in the higher turbulence intensity. This could lead to some variations in the expected responses. The seeds where analysed, to verify that they would be useful in the project, by using statistics, the defined seeds in Table 4.3 (p. 23), were found suitable.

When this project started the version of FAST that was used, was version 6, in the middle of the project it was decided to use the newest version which is version 8. An assessment was done to see if the two version would give the same responses it was concluded that the two versions where for the most identical.

The knowledge gathered from the analysis of the turbulence intensity Chapter 3 (p. 11) was used to determine the numerical values of the turbulence intensity. The wind shear values, were chosen by aid from the supervisors. The air density minimum value and maximum value for picked with help from previous reports about wind climate parameters, Toft et al. [2000]. The Design load cases (DLC) considered in this report are 1.2 which considers fatigue, and 1.3 which applies ETM, and considers ultimate analysis.

The new method in IEC 64100 ed4. Which states that for the blades the average values of a 10 minutes simulation should be multiplied by a factor 1.35, and for the other components the characteristic value is obtained by the largest (or smallest) among the 99th percentile of a 10 minutes simulation and multiplied with factor 1.2. This new method usually estimated a higher response than load extrapolation.
In DLC 1.2, rainflow counting was used to estimate the number of cycles and stresses.
The 4 components that are considered are described in Table 2.4 (p. 10)

Two methods for establishing response surfaces were considered, Comparing Central Composite Design (CCD), and Taylor to create the models for NREL 5 MW turbine, resulted in a better model with CCD, where the Taylor expansion method usually resulted in higher values than the simulations estimated. The CCD models tend to follow the simulations surfaces.

A load sweep with three climate parameters, the turbulence, wind shear and the air density, resulted in odd responses. It was not expected that the air density would have as much change as it did. This does not comply with the expectations that the project group anticipated. The responses increase with increase in the turbulence intensity as expected.

To assess if the model produces reliable result, the new DTU 10 MW wind turbine Michael Borg [2015] was benchmarked to the NREL 5 MW wind turbine Jason M. Jonkman [2005]. The turbulence intensity and wind shear, were used to make the surface graphs. From the surface graphs it can be concluded that the DTU 10 MW wind turbine is exposed to higher responses as is to be expected has it as larger physical dimensions. For the components individuality the RootMyb1 shows the same trend, increase in responses to rated wind and thereafter the pitching of the blades starts to reduce the response. For RootMxb1, DTU 10 MW wind turbine varies bit from the NREL 5 MW as it does not show high values in above rated wind speed. The TwrBsMyt for the DTU 10 MW turbine does not increase as the NREL 5 MW turbine. For LSSGagMxa the responses close to the rated wind speed are similar. But after that the responses do not rise as in NREL 5 MW turbine.
There were problems in getting the simulations for the DTU 10 MW turbine to produce reliable responses and therefore some changes were made as mention in Chapter 6 (p. 47), were the initial rotor speed was changed for below rated wind speed and above rated wind speed, and lowered even more for the two highest wind speed. It is uncertain if that has

had any influences on the responses.

The load sweeps for the DTU 10 MW turbine, showed more variation in the responses than NREL 5 MW turbine. It was decided to only go up to 30 %, with the turbulence intensity. As the simulations had shown some numerical instability for the high turbulence intensity. Otherwise the CCD follows the simulations well.

For the uncertainty analysis the aim is to assess the sensitivity of the climate parameters. It was expected that the turbulence intensity is the most sensitive, and then wind shear. After the calculations this was confirmed. The parameters from the Weibull distribution A and k did not have significant important for D.L.C 1.3 however they did for D.L.C 1.2. See results below.

Table 9.1: Results from uncertainty analysis. Case 1-6.

Variance/(DLC)	Case 1	Case 2	Case 3	Case 4	Case 5	Case 6
$V_{\sigma CCD}$ (1.2)	0.149194	0.421458	0.283762	0.283766	0.283764	0.283764
$V_{\sigma CCD}$ (1.3)	0.282563	0.285165	0.283072	0.284441	0.280823	0.291748

Table 9.2: Results from uncertainty analysis. Case 6-12.

Variance/(DLC)	Case 7	Case 8	Case 9	Case 10	Case 11	Case 12
$V_{\sigma CCD}$ (1.2)	0.008113	0.008116	0.008101	0.008136	0.008114	0.008115
$V_{\sigma CCD}$ (1.3)	0.008113	0.008117	0.008114	0.008114	0.008114	0.008114

The results for DLC 1.3 do not differ much, with a further analysis they could be verified. As these analysis shows, the responses depend on the different climate parameters and there extreme values. Using models instead of simulations could be useful in some cases, but should be done with caution, as for an example if using Taylor one would get higher responses than a simulation would give. In some cases the use of CCD does the same. The models are subjected to some uncertainties, and less accuracy compared to the aero elastic simulations. More data should be considered for generating reliable response models. The result form the uncertainty analysis represent the uncertainty related to site assessment, when combined with the uncertainty related to structural aero dynamics and resistance, and a limit state equation is formulated, a reliability analysis could be achieved.

Bibliography

B. M. Ayyub & R. H. McCuen (1997). *Probability, statistics and Reliability for Engineers and Scientists.* Handbook. CHAPMAN & HALL/CRC.

Energi Styrelsen (2015). *Energi Styrelsen.* Internet. URL : http://www.ens.dk/. 26-10-2015.

L. M. Fitzwater (2002). *Environmental Contours for Wind Turbines, Considering a Lognormal Distriubtion for Turbulence.* Handbook. Research.

IEC (2005). *International Standard IEC-61400-1: Windturbines: Part 1- Design requirements.* Handbook. IEC.

M. L. B. J. Jason M. Jonkman (2005). *FAST User's Guide.* Technical Report. NREL.

Z. Liu & P. Frigaard (2001). *Generation and analysis of random waves.* Report. Aalborg University.

H. B. Michael Borg, Mahmood Mirzaei (2015). *Qualification of innovative floating substructures for 10MW wind turbines and water depths greater than 50m.* Technical Report. DTU.

J. Schjødt-Thomsen (2015). *Fatigue.* Lecture. Aalborg University.

J. D. Sørensen (2005). *External Conditions.* Handbook. Aalborg University, Department of civil engineering.

H. S. Toft, et al. (2000). *Wind Climate Parameters for Wind Turbine Fatigue Load Assessment.* Handbook. Aalborg University, Department of civil engineering.

H. S. Toft, et al. (2015). *Assessment of wind turbine structural integrity using response surface methodology.* Handbook. Aalborg University, Department of civil engineering.

Appendix A

Intern Appendix

A.1 Wind Turbines

In this section the properties for the NREL 5 MW wind turbine and the DTU 10 MW wind turbine will be described. When the two wind turbines are benchmarked against each other the idea is to study how response behave. It is expected that the response of the DTU 10 MW will be higher since the physical dimensions of the 10 MW turbine are larger.

NREL 5 MW Turbine

The properties for the 5 NREL MW wind turbine can be seen in Table A.1

Table A.1: Properties for the NREL 5 MW wind turbine.

Rating	5 MW
Rotor Orientation, Configuration	Upwind, 3 Blades
Control	Variable Speed, Collective Pitch
Drivetrain	High Speed, Multiple-Stage Gearbox
Rotor, Hub Diameter	126 m, 3 m
Hub Height	90 m
Cut-In, Rated, Cut-Out Wind Speed	3 m/s, 11.4 m/s, 25 m/s
Cut-In, Rated Rotor Speed	6.9 rpm, 12.1 rpm
Rated Tip Speed	80 m/s
Overhang, Shaft Tilt, Precone	5m, 5º, 2.5º
Rotor Mass	110,000 kg
Nacelle Mass	240,000 kg
Tower Mass	347,460 kg
Coordinate Location of Overall CM	(-0.2 m, 0.0 m, 64.0m)

DTU 10 MW Turbine

The properties for the DTU 10 MW wind turbine can be seen in Table A.2

Table A.2: Properties for the DTU 10 MW wind turbine.

Rated Power [MW]	10.0
Rotor Orientation, Clockwise rotation	Upwind
Control	Variable Speed, Collective Pitch
Drivetrain	Medium Speed, Multiple-Stage Gearbox
Rotor, Hub Diameter	178.3 m, 5.6 m
Hub Height	119.0 m
Cut-In, Rated, Cut-Out Wind Speed	4 m/s, 11.4 m/s, 25 m/s
Cut-in, Rated rotor speed	6 RPM, 9.6 RPM
Rated Tip Speed	90 m/s
Rotor Mass	227.962 kg (each blade 41 tons)
Nacelle Mass	446,036 kg
Tower Mass	628,442 kg
Number of blades	3
Gearbox ratio	50
Blade prebend [m]	3.332
Overhang, Shaft tilt, Pre-cone	7.07 m 5°, -2.5°

A.2 Fast Analysis

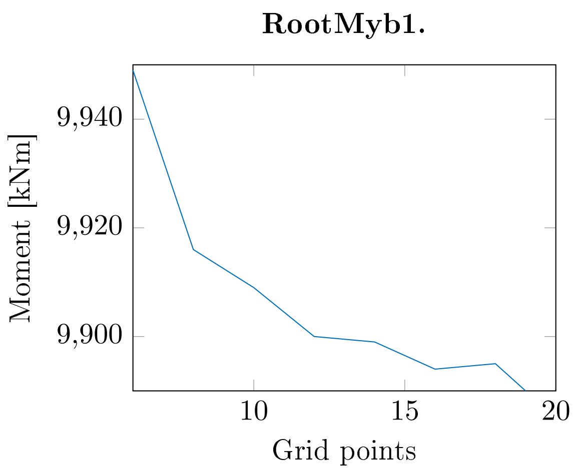

Figure A.1: Blade root flapwise moment.

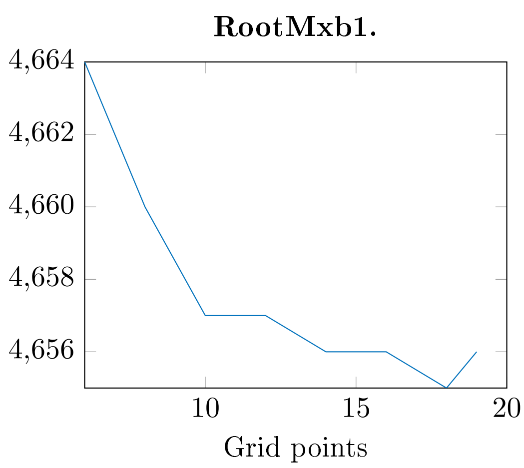

Figure A.2: Blade root edgewise moment.

[H]

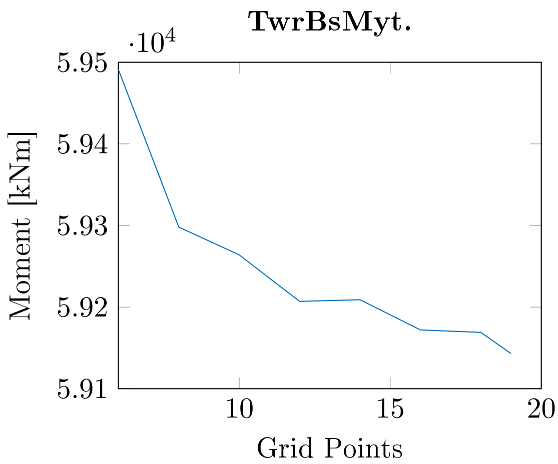

Figure A.3: Tower bottom for-aft bending moment.

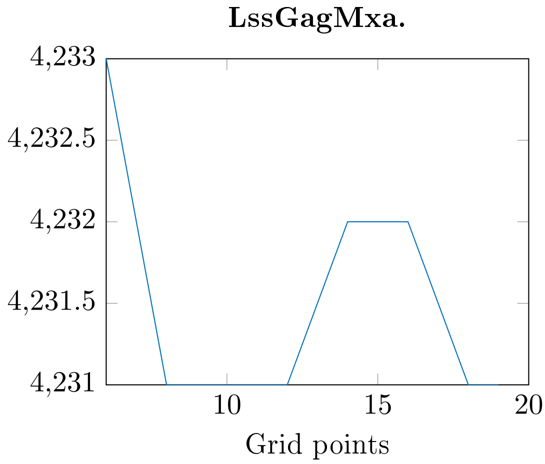

Figure A.4: Low speed shaft torque.

It is seen from Figure A.1 A.2 A.3 and A.4 that the response will decrease while increasing the the grid point. and those components follow the same trend. However for Figure A.4 the trend of the curve diverge from the rest of the components, but the response change is very small.

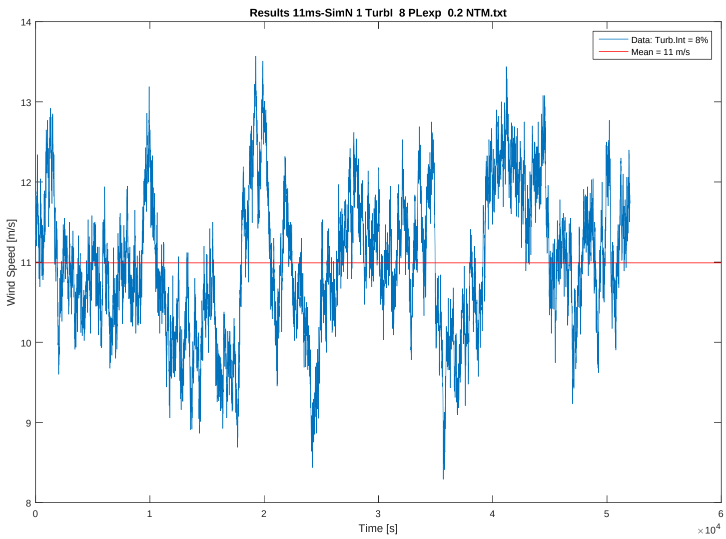

Figure A.5: Simulated time series of wind speed in FAST for mean wind speed 11 m/s

For Figure A.5 the applied turbulence intensity is 8 % and the calculated turbulence intensity from the time series is 8 %.

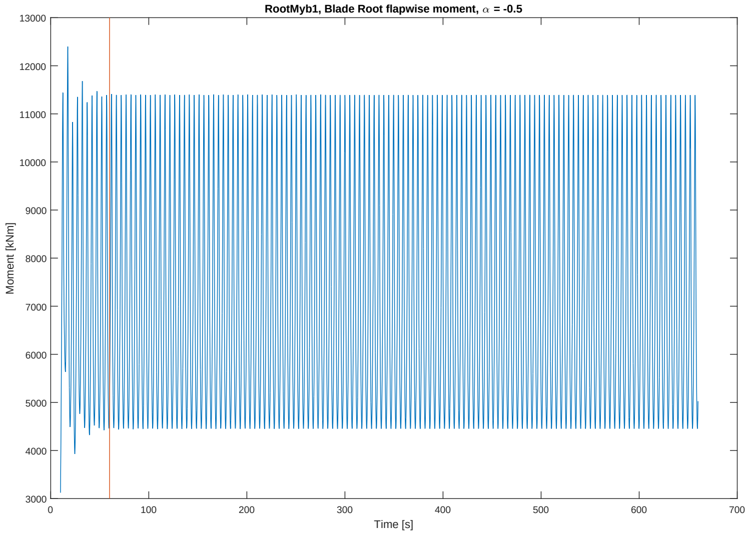

Figure A.6: Time series for mean wind speed 12, turbulence intensity of 0 and wind shear of -0.5

A.3 Comparing V6 and V8

The responses are the mean value of the seeds.

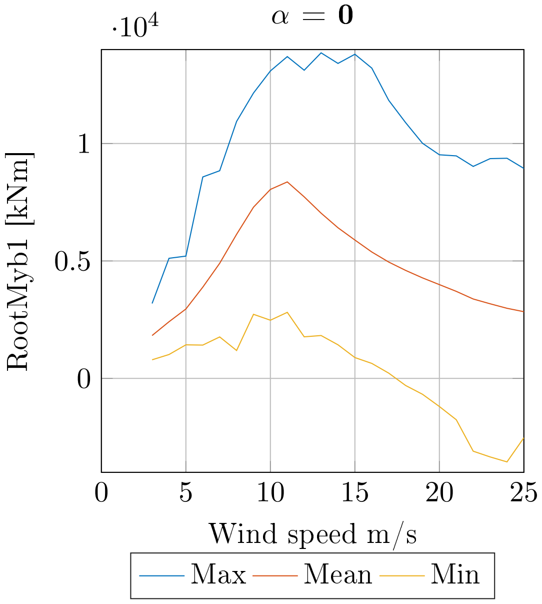

Figure A.7: Flapwise bending moment V6.

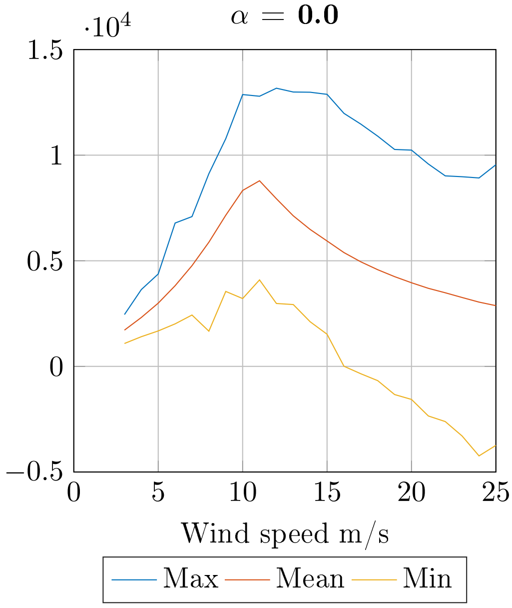

Figure A.8: Flapwise bending moment V8.

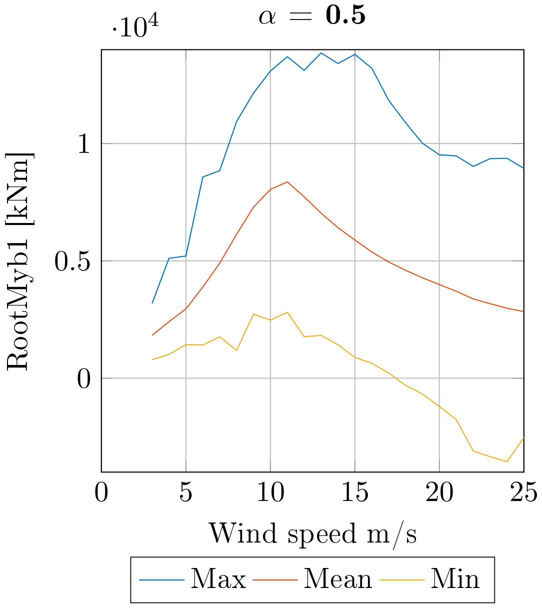

Figure A.9: Flapwise bending moment V6.

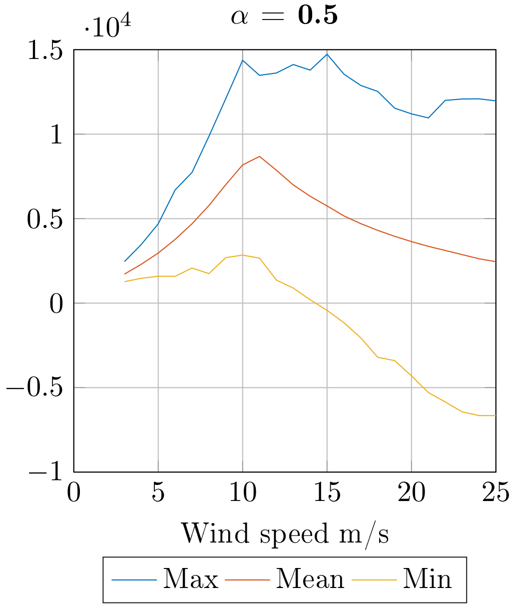

Figure A.10: Flapwise bending moment V8.

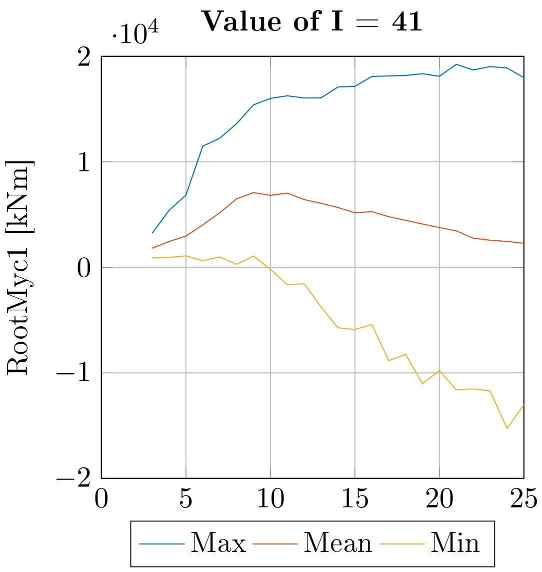

Figure A.11: Flapwise bending moment V6.

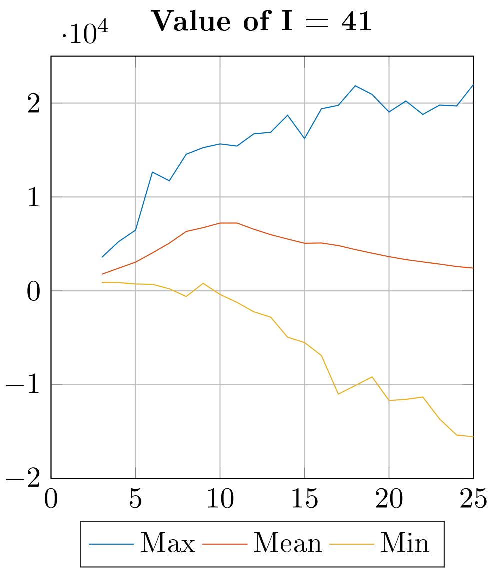

Figure A.12: Flapwise bending moment V8.

A.4 NREL time series

An example of output for NREL 5 MW at 24 m/s at 91 %.

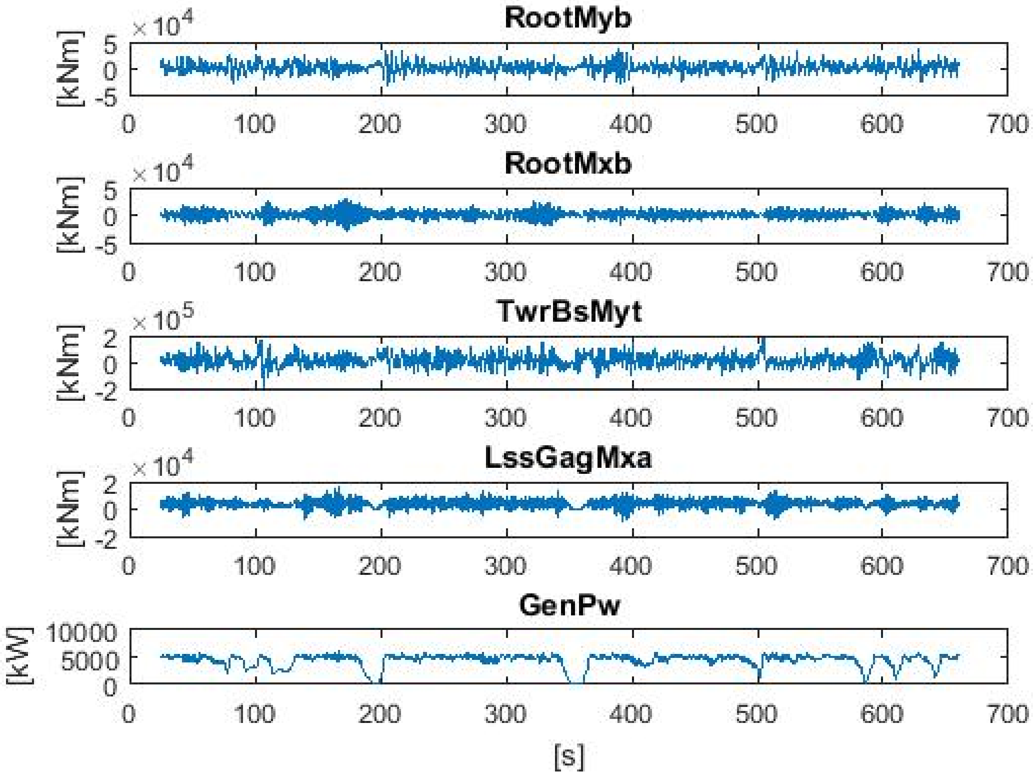

Figure A.13: Power output

A.5 DTU power output

A small comparison between the power out put when the climate parameters are changed.

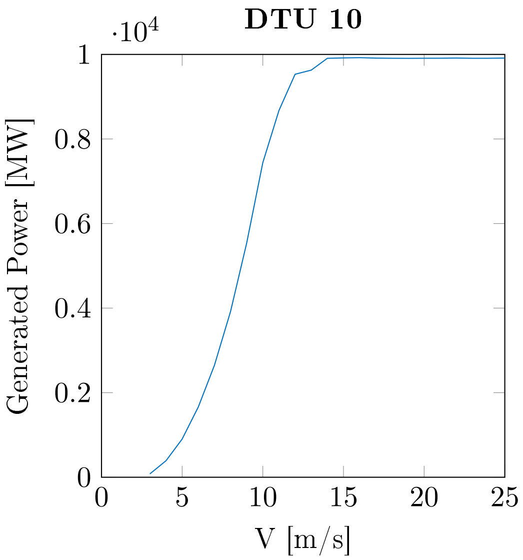

Figure A.14: Wind shear 0.0 Seed 1.

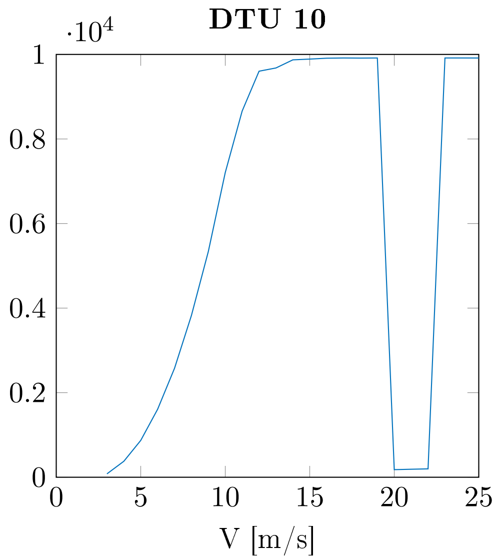

Figure A.15: Wind shear 0.4 seed 14.

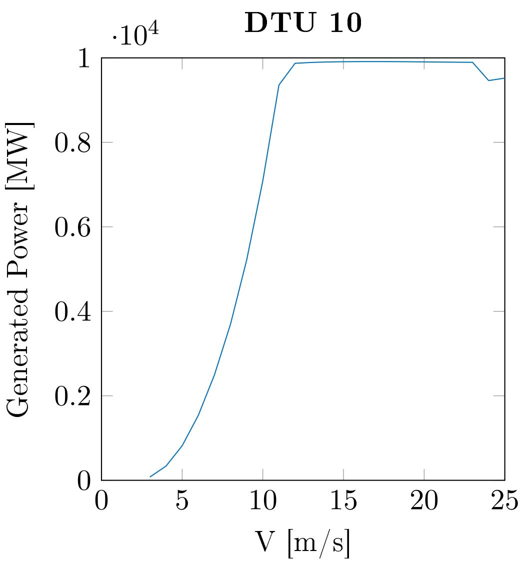

Figure A.16: Turbulence 0 % Seed 1.

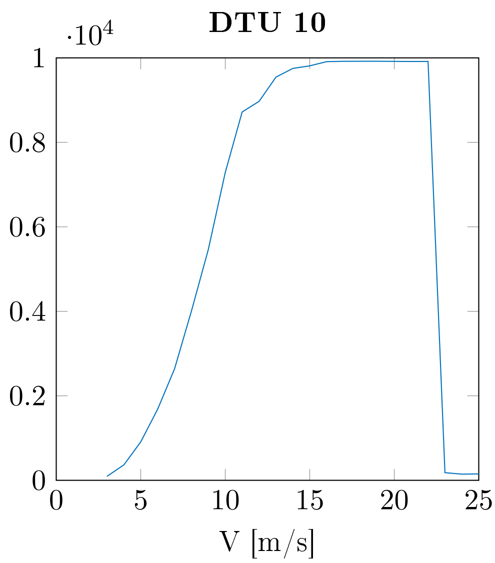

Figure A.17: Turbulence 24 % Seed 3.

The majority of the seeds generated the acceptable power output. The mean values of all the seeds for both the wind shear and turbulence can be seen in B.

Appendix B

External Appendix

- DTU 10 MW
  - Generated power
    - Alpha
    - Turbulence
  - Models
    - Load Sweep
  - Regression Parameters
    - Load Sweep
  - Turbulence Variation
    - LSSGagMxa
    - RootMxb1
    - RootMyb1
    - TwrBsMyt
  - Wind Shear Variation
    - LSSGagMxa
    - RootMxb1
    - RootMyb1
    - TwrBsMyt
- NREL 5 MW
  - Models
    - Load Sweep 1
    - Load Sweep 2
    - Load Sweep 3
  - Regression Parameters
    - Load Sweep 1
    - Load Sweep 2
    - Load Sweep 3